

Calculations of Energetic Ions Energy Transfer via Slowing down Mechanism



Ghulam Murtaza

**Department of Physics
Quaid-i-Azam University Islamabad, Pakistan
(2017-19)**

This page [is] intentionally left blank.

Dedicated to
my beloved parents, sisters
and brother

Calculations of Energetic Ions Energy Transfer via Slowing down Mechanism



Ghulam Murtaza

Submitted in partial fulfillment of the requirement
for the degree of Master of Philosophy in Physics

**Department of Physics
Quaid-i-Azam University Islamabad, Pakistan**

Certificate

This is to certify that the work contained in this thesis entitled **Calculations of energetic ions energy transfer via slowing down mechanism**, was done by **Ghulam Murtaza**. It is fully adequate, in scope and quality, for the degree of **M.Phil Physics**.

Supervisor: _____

Dr. Majid Khan
Department of Physics
Quaid-i-Azam University Islamabad

Chairman: _____

Prof. Dr. Nawazash Ali Khan
Department of Physics
Quaid-i-Azam University Islamabad

Acknowledgments

All the praises are for the **Almighty Allah**, the most gracious and merciful of all. I want to offer special thanks to my supervisor **Dr. Majid Khan** for his support, guidance, and excellent supervision. I want to thank my friend and senior research fellow **Mr. Muhammad Zia** for being helping and supportive. Special thanks to all my classmates for their valuable suggestions and encouragement. I am grateful to my dear friends **Ahmad Raza, Faizan Ullah Khan, Imran Hussain, Hamza Abbasi, and Shamsheer Ali Wattoo** for their love and support. I am indebted to my beloved parents for their love, prayers, and support. I must offer thanks to my beloved siblings and dear friends for supporting me throughout my career.

List of Figures

3.1	Scheme for Δv_i	28
3.2	Graph for zero and maximum energy transfer.	37
3.3	A comparison of different critical parameters	41
3.4	Energy deposition curves vs Injection energy	43
3.5	Energy deposition curves vs T_e	44
3.6	Slowing-down time of ions	45
3.7	Slowing-down velocity of ions	46
3.8	Relative particle losses vs density ratio	47
3.9	Relative energy losses vs density ratio	48

Contents

Acknowledgements	v
Abstract	vi
1 Introduction	1
1.1 Effect of different perturbations on fast ions losses	2
1.2 Interaction between energetic fast ions and sawtooth oscillations	4
1.3 The fast ion D_α diagnostic: An application of fast ions	6
1.4 Slowing-down of energetic fast particles	7
2 Derivation of kinetic equation	9
2.1 The statistical point of view	9
2.2 The distribution function	10
2.2.1 Time evolution of the distribution function	12
2.3 Liouville equation	13
2.4 S-particle distribution function	14
2.4.1 BBGKY-Heirarchy	16
2.5 Cluster expansion	20
3 Slowing down by small angle Coulomb collisions	24
3.1 Slowing down of fast ions	32
3.2 Another derivation for mean rate of energy transfer	36
3.3 Energy transfer (from zero to maximum)	37
3.4 Time of Thermalization	39
3.5 Equilibrium temperature of a two-component plasma	42
3.6 Results and Discussion	42
Bibliography	49

Abstract

Fast ions in various toroidal devices, such as in tokamaks, play a vital role in bringing and sustaining a thermonuclear fusion process. They can transfer their (excessive) energy to the bulk plasma particles via various collisional processes, for example, the so-called slowing-down process. Here we have considered the slowing-down of energetic ions generated by neutral beam injection in a tokamak plasma has been studied. The kinetic theory of plasmas, which involves the time evolution of various species' phase-space distribution function, has been employed. First, we have presented a detailed derivation of kinetic equations and introduced the concept of Fokker-Planck collisional effects.

The injection of fast neutral atoms is the most exciting method for auxiliary heating, via the transfer of collisional energy from the fast ions formed in the limited orbits of the fusion plasmas' plasma particles. Particles and energy losses due to charge exchange with the energy transferred to plasma ions, electrons, and background neutrals are calculated. Since the losses of energy transfer and charge exchange depend strictly on the neutral density and the electron temperature, the allowance of arbitrary profiles for $n_0 = n_e$ and T_e and the fast ion accumulation are also included.

The energy transferred to plasmas can be severely affected by charge exchange between fast ions and neutral background particles. Coulomb scattering is mainly used to find the velocity distribution of fast ion populations. The transport of high-speed ions is generally much slower than thermal transport, except during MHD events. Intensified populations of fast ions drive collective instabilities.

Chapter 1

Introduction

The understanding of fast (or energetic) ions behavior in various fusion devices is an essential need for a successful energy producing reactor. Since these particles have an importance in future burning plasmas. Undoubtedly, these can provide a prime source of heating to continue the condition of self-ignition. Thus, for an ignited fusion reactor, it is necessary to have a satisfactory confinement of the fast ions [1-5]. If the alpha particles, born due to D-T reaction, are considerably lost from the plasma due to some reasons, the condition of self-ignition is surely abolished. The localized heat load is faced by the plasma facing components of reactors and can appear as a source of compelling vaporization and melting of various components facing plasma. Due to this, realization of the physics problems relevant to fast ions is a central in the struggle to accomplish secure utilization of a fusion reactor for energy production.

The principle subjects of fusion plasma theory and experiment are the confinement, thermalization and diffusion of the beam of fast ions injected neutrally [6]. Studying the process of slowing down of the fast ions injected via neutral beam relevant to both thermal background plasma and the confinement of the fast ions are therefore critical and is significant. The beam ions are defined in the following way. The ions which have the velocity v_b greater than the thermal velocity of the background plasma ions v_i and less than the thermal velocity of the background plasma electrons v_e , i.e., $v_i \ll v_b \ll v_e$, are known as the beam ions. The other condition is on the density of the fast ions. The density of the fast ions n_b is less than the density of the background plasma n in tokamak plasma, i.e., $n_b \ll n$ which

is known as weak-beam approximation. As a result, these neutral beam injected (NBI) fast ions can play the role of test particles that are slowed down and diverted because of numerous Coulomb collision with the background plasma. By the study of the classical transport theory, we can understand the above mentioned process [7-9]. In a fusion plasma which is restrained magnetically, the rate of slowing down of the NBI fast ions actually provides the rate of heating and the transferred energy from the NBI to the background plasma [10]. Different techniques are used to limit plasma to the volume of the reaction at a certain temperature. One of them is the fusion reactor, Tokamak, which works on the concept of magnetic captivity [11]. In this scheme, magnetic fields are employed to command the orbital motion of the plasma components. The word Tokmak comes from the Russian language and it stands for "toridal'naya room s magnetanimi katushkami" which means toridal chamber with a magnetic coil used in toridal incarceration. Tokamak was developed by Soviet plasma physicists in the 1960s [12] and is considered the most advanced and well-studied fusion concept. The most recent of that is the well-known International Thermonuclear Experimental Reactor (ITER) which is under construction in France [13,14]. For the more technical and academic details about ITER we refer the reader to www.iter.org.

1.1 Effect of different perturbations on fast ions losses

Unless the plasma is heated to a certain temperature, it is unimaginable to obtain a nuclear fusion reaction such that the thermal energy overcomes the corresponding Coulomb barrier among positive nuclei. In the center of tokamak, through radio frequency (RF) heating and fusion-generated alpha particles, it is essential to capture high-energy ions produced by NBI [15]. Fast ions such as alpha particles, which are formed in fusion reactions, have the steady velocity vector at 3.5 MeV [16]. However, fast ions formed by NBI and ion cyclotron resonance heating (ICRH) contain only specific directed vectors. Whereas, the energetic ions having velocity vectors normal to \mathbf{B} are produced via ICRH mechanism. It is a technique in which plasma ions are speed up by electromagnetic waves to a certain limit of many hundred keV at their corresponding gyro frequency. In NBI (the process in

which plasma heating is by injection of a plasma beam), the velocity vector is dependent on the geometry of the NBI and the change in its velocity. Since there is no effect of electric and magnetic fields on neutral particles, thus, the NBI cannot be affected by such fields of tokamak. Fast ions play a very important role in achieving an easy state of plasma burning, however, the loss of energetic ions is caused by various mechanisms, e.g. first orbit losses, scattering, collective plasma instability and diverse transport modes [17,18].

The lost portion of energetic ions can be assessed adapting different kinetic approaches via evaluating the transport coefficients out of which coefficient for radial diffusion (perpendicular to the flux surfaces in which the magnetic field lies) is an essential one. To calculate the radial diffusion accurately, the exact knowledge of the particles trajectories is necessary. For which different numerical methods are employed to evaluate the trajectories, followed by the transport coefficients of fast ions as affected by tokamak perturbations [19].

In order to analyze the conduction of high-energy ions in current (e.g. JET) and future (e.g. ITER) tokamaks, it is extremely important to have complete knowledge of fast ion orbital motion and losses [20-22]. As a conclusion of theoretical and experimental observations, it turns out that alpha particles generated via axisymmetric magnetic field model of high-current tokamak D-T reactor, can be confined, and, thus, play an important part to provide the heat required to take the tokamak plasma (self-heating effect) to the temperatures necessary for fusion [23,24]. Nevertheless, specific, intermittent and otherwise, such as toroidal field (TF) waves and magnetic hydrodynamics (MHD) methods, these perturbations may cause fast ion loss from tokamak [25]. These losses occur through various resonance interactions, e.g. there can be resonance loss of banana (trapped particles due to mirror effect in tokamak magnetic field, executing a periodic motion) particles due to TF ripple periodicity. Likewise Alfvén waves (having almost the same velocity as fusion born alphas) can resonantly interact with these particles thus contributing in the loss of these fast ions. The fast ions, which have a relatively low energy, can also interact resonantly with low frequency MHD modes, e.g. neoclassical tearing modes. The resonance condition is $\omega_{D/f} = \omega$. The particles with energy $E_{f/i}/T_{i/l} \approx 2Rl/r_{pl}$, where r_{pl} is the length of the corresponding thermal ion pressure gradient, are able to satisfy the condition of $\omega_{D/f} = \omega_{il}$.

Here ω_i is the diamagnetic frequency of the thermal ion. In present day experiments, the energy range of a fast ion of this regime is 100 keV, which is a typical value of NBI ions.

Thus, the resonant interaction of fast ions with low frequency MHD modes can be the source of destabilization of internal kink modes [26,27]. It is thought that the physical phenomenon of fishbone instability [22] occurs due to this resonant destabilization. The name, fishbone instability, comes out from the characteristic experimental trace of the related magnetic fluctuation bursts. The phenomenon of resonant interaction of fast ions is prominent not only when the energy of fast ions is in the range of 100 keV, but also when the density of fast ions have a value above a critical threshold. Above this critical threshold a new continuum Alfvén mode becomes unstable. When this happens, the rate with which energy is transferred from the fast ions to the different modes is also enhanced [27]. It is observed that the rate of energy transfer becomes larger than the damping rate of background continuum.

1.2 Interaction between energetic fast ions and sawtooth oscillations

For a D-T born alpha particles' radial redistribution due to sawteeth is studied on TFTR tokamak with the pellet charge exchange diagnostic [28,29] and alpha-CHERS [30]. It is observed that the loss of alpha particles due to sawtooth collision is very small. The NBI and D-D tritons both appear to be reorganized due to sawteeth in JET [31]. Nowadays it is thought that the particles with higher energy have lesser chance of disturbance due to sawteeth, and effect of sawteeth on the fast energetic particle depends on the type of sawteeth. We can find a lot of theoretical explanations of the redistribution of the fast energetic particles which show up because of a sawtooth collision [32,33].

The transport of alpha particle can be enhanced due to interaction between sawteeth and many other single-particle alpha effects. As an example we can quote the significant reorganization of alpha particles which occurs in ITER from the inside to the outside of the

inversion radius at $r'/a' \approx 0.5$ due to a sawtooth. This leads to a considerable enhancement in toroidal field ripple-caused alpha particle heat loss onto the wall. Even though the reorganization of a large number of alpha particles due to a considerable sawtooth collision is predicted in ITER, it is possible that the ignition will sustain because the time required for the alpha particles' relaxation (~ 1 sec) is less than the rate of loss of plasma energy (~ 5 sec). With the help of TRANSP code [34], simulations have been done to study the effects of TF ripples sawtooth on alpha particles in ITER. In ITER, the biggest fast ion losses in toroidal Alfvén eigen-mode activity were predicted [35].

On the contrary, for a definite period of confinement, the energetic fast ions are able to suppress the sawtooth oscillations. The sawtooth-free period being definite by the extension of the locality where $q < 1$, up to the point where $q = 1$. Here q denotes the safety factor [36]. At $q = 1$, approximately half of the minor radius of plasma is approached. These long lasting "monster sawteeth" are defined by the congestion of the temperature and pressure portrait well before the sawtooth collision happens. It shows that the internal kink instability threshold is approached as a result of the current density's transformation. In case of JET, the sawtooth-free period of between one to five seconds have been achieved in discharges with intensified ICRH. A very few number of ions approach energy in the range of MeV [37]. Same results are have been achieved in TFTR and other tokamaks. A little sawtooth stabilization is also observed in many other tokamak discharges with NBI fast energetic ions. Even though it is challenging to get a huge prolonging of the sawtooth duration NBI heating in present day experiments. The results obtained of these experiments shows a good agreement with theoretical predictions of internal kink stabilization via fast energetic ions .

If ignition is observed in ITER, alpha particles obtained through fusion are supposed to abolish sawteeth transiently. It can happen for periods that are high enough on the energy confinement time scale. In case of supposition that the sawtooth-free period in ITER is defined with the help of extension of the q profile as in JET. With the extrapolation of the results obtained from the JET shows that the long-lasting monster sawteeth with periods of the order of 100 s are achievable in ignited ITER discharges. This judgment can be justified with the help of simulations. There are many numerical MHD codes, which

incorporate the kinetic effects of the fast energetic particles as well as those of thermal ions [38]. Nonetheless, this suppression of the sawtooth transient can be useful in granting for peaked profiles and an enhanced limit of ignition, the considerable crashes related with the elongated period of time are a point of interest.

1.3 The fast ion D_α diagnostic: An application of fast ions

In most of magnetic fusion experiments hydrogenic superthermal energetic ions are a part. These energetic ions are introduced via neutral beams or via wave heating process. Various aspects of the nature of plasma are difficult to understand without the prior knowledge of the distribution function of the fast ions.

Nowadays a new mechanism has developed as a persuasive diagnostic of the distribution function of the fast ions. This mechanism, namely, fast ion D_α (FIDA), takes advantage of visible light given off by energetic deuterium ions as they move forward through a neutral beam. An analogous analysis of energetic helium ions was done in 1990s. A FIDA measurement is known as an application of a phenomenon, namely, charge exchange recombination spectroscopy [39]. The process through which this measurement is carried out is as follows. The act of charge exchange takes place when a deuterium ion orbits through a neutral beam. Due to this event the fast ion is neutralized. As there is no charge on a neutral ion, so it will follow a straight line trajectory. Generally the energetic fast ion exist in an excited atomic state. As it moves, its atomic state is changed due to collision with the plasma or it shows a radiative decay. We know that a transition between $n = 3$ to $n = 2$ level is known as a Balmer- α transition, for which a visible D_α photon is emitted.

The light emitted as a result of Balmer- α transition shows a huge Doppler shift. This spectral shift is utilized to discriminate the FIDA emission from the remaining luminous light sources of D_α . The central technical problem is the background's subtraction. It is observed that a diagnostic which is done through spectroscopy commonly accomplished temporal, energy, and transverse spatial resolution of approximately 1ms, 10 keV, and 2 cm, respectively. Those installations which use narrow band filters attain immense spatial and temporal resolution at the price of spectral knowledge. In order to achieve high spectral

resolution, the bandpass-filtered light passes straight through a photomultiplier. It allows the detection of about ~ 50 kHz vibrations in FIDA signal. To achieve a 2D spatial portrait, it is suggested that the bandpass-filtered light should pass through a charge-coupled device camera. In this way we will be able to get comprehensive images of fast ion reorganization which occurs at instabilities [40].

The FIDA signals, which are measured with the help of qualitative and quantitative models, are compared with the distribution function of fast ions. A good agreement between theory and experiment is obtained in beam heated MHD-quiet plasmas in our first quantitative testings. It is interesting to know that FIDA diagnostics are nowadays functional at magnetic fusion sites around the globe. They are utilized to understand acceleration of fast ions via ion-cyclotron heating, to measure the transport of fast ions via MHD modes and microturbulence. They are also used to analyze instabilities which are driven by fast ions.

1.4 Slowing-down of energetic fast particles

To achieve the purpose of additional heating in today's tokamak plasmas, one of the most auspicious and well proven technique is the injection of fast neutral atoms. There occur collisions between the fast ions borne on confined trajectories and the plasma particles. These collisions are the source of energy transfer from fast ions to the plasma particles. Because of this collisional energy transfer a heating effect is produced in the tokamak. As a result slowing-down of fast ions takes place. The experimental results of the slowing-down process are in good agreement with classical neutral beam injection (NBI). The process of energy transfer is vigorously distressed due to charge exchange phenomenon between fast ions and background plasma's neutral particles.

The formulae given in chapter 3 are used to describe the time of rapid ions depletion from their initial energy to thermal energy [41]. At the critical energy, the exchange of differential energies in ions is equal to that of electrons. For a plasma which has only one dominant species and not too much high Z_{eff} belongs to the following: $Z = (1/n_e) \sum_j n_j Z_j^2 (A_i/A_j) \simeq 1$. This means that the level of impurity in plasma does not have

too much affect on the critical energy and slowing down time. In all numerical calculations, thus, $Z = 1$ is supposed.

Since we are associated with the energy dependence of fast ion numbers, it must be understood that the equations we will use are summed over the pulse of a neutral beam. $N_0 = N(E_0)$ gives the number of fast ions with initial energy E_0 produced during a pulse period. To obtain the value of $N(E)$, the number of fast ions that are always available at energy E ($E_0 > E > T$), it is supposed that, firstly all fast neutrals produced by charge exchange processes will leave the plasma and, secondly that it is the only loss mechanism for the fast ions.

Plasma-escaping fast charge exchange neutrals represent a source of impurities entering the plasma after forming heavily impure atoms on the walls. It is supposed that the equations for slowing down velocity and for the particle loss rate also hold for all energies down to the ion temperature. As long as $E_0 \gg T_i$, deviating from these assumptions does not play a vital role.

The change in the total energy of high speed ions, passing the energy interval dE , is due to two reasons, energy transfer in the background plasma and energy losses associated with particle losses. There are also energy-related losses from the charge exchange process during slowing down time.

The main objective of this work is to compute the related energy losses due to the collision between the species mentioned above. In our calculations for slowing down of fast ions, we assume a Maxwellian background plasma.

Chapter 2

Derivation of kinetic equation

In this chapter we shall review one of the most important plasma approach, namely, the kinetic theory. In this regard a step by step derivation is provided. We start with a general statistical N-body distribution function and, by proper integrations, derive the one particle distribution function.

2.1 The statistical point of view

In plasma, there are a large number of charged particles that are important for long and short distance forces and give rise to the cumulative behavior of particular complicated systems. For analytical explanations, the combined effect of these time-dependent electromagnetic forces is extremely complicated, therefore many other methods have been proposed to deal with the microscopic features associated with these systems.

Let us assume that N identical particles are in motion in a plasma and each particle is characterize by its corresponding Newtonian equation, i.e. for $i = 1, 2, 3, \dots, N$ then we can write

$$m\ddot{\mathbf{R}}_i(t) = F_i(t) \tag{2.1}$$

$$\Rightarrow \ddot{\mathbf{R}}_i(t) = \frac{F_i(t)}{m}, \tag{2.2}$$

considering that m is the mass of the particle, $\mathbf{R}_i(t)$ is the position vector of the i th particle,

and $F_i(t)$ is the force experienced by the particle at any time t . The interaction of i th particle with all other particles present in the system is included in Eq. (2.1). The solution of such N equations is obtained by integration such that

$$\dot{R}_i(t) = \dot{R}_i(0) + \frac{1}{m} \int_0^t F_i(t') dt' \quad (2.3)$$

and

$$R_i(t) = R_i(0) + \frac{1}{m} \int_0^t dt' \int_0^{t'} F_i(t'') dt'' \quad (2.4)$$

The equations above give the behavior of a particle in plasma, nevertheless, it is not practical to integrate these for each particle interacting with all other particles. Generally, F_i contains velocities and positions of all plasma particles. Even though the forces through which the particles are interacting are not complicated and integration is executable, but still it is difficult to solve for N -particles.

The motion of the particles is described by the Eq. (2.1). Due to large number of particles and less information about the initial conditions, solution of Eq. (2.1) for each particle is a difficult job. With the help of super-computers that have large computational power, and using the codes like particle in a cell (PIC), the number of particles that can be followed is still well below the actual value of N [42]. The dynamics of the particles can be described statistically for which the kinetic description is used and is also known as the Transport theory. The transport equation is a probabilistic description which includes the collisional effects, the distribution function of the particles, and the source term, if any. In such an approach the identity of individual particle is not important and we are interested in an average behavior of the system.

2.2 The distribution function

The distribution function $f(r, v, t)$ of the particles is the main element in kinetic theory. It is known as the density of phase space, that is, the number of particles per unit volume of phase space. By using the statistical approach, we can study the dynamics of a system

which consists of N particles at any time t , with velocities v_i and position vectors r_i . To define the probability function, we need the distribution function of the particles. The exact distribution function of above mentioned system can be written as

$$f(\vec{r}, \vec{v}, t) = f_N^{ex}(r_1, v_1, r_2, v_2, \dots, r_N, v_N, t). \quad (2.5)$$

It describes that the particle which have the velocity v_1 lies at position r_1 , the particle which have the velocity v_2 lies at position r_2 , and same holds for the remaining $N - 2$ particles with their corresponding velocity and position coordinates. Therefore, the distribution function of $6N$ dimensions can be written by using exact positions and velocities via Dirac delta function as follows [43]

$$f_N^{ex}(r_1, v_1, r_2, v_2, \dots, r_N, v_N, t) = \prod_{i=1}^N \delta[r_i - R_i(t)] \delta[v_i - \dot{R}_i(t)]. \quad (2.6)$$

The phase space consists of $3N$ spatial coordinates and $3N$ velocity coordinates, meaning a $6N$ dimensional phase space denoted as the Γ - space.

To keep the things simple, we introduce the following notations

$$(x_1, x_2, \dots, x_N) = X, \quad (2.7)$$

$$(v_1, v_2, \dots, v_N) = V, \quad (2.8)$$

with

$$(X_i, V_i) = r_i, \quad (2.9)$$

$$[X_i(t), V_i(t)] = R_i(t). \quad (2.10)$$

These abbreviations are used to simplify the expression of the distribution function.

2.2.1 Time evolution of the distribution function

The distribution function, after using the above definitions comes out to be

$$f_N^{ex}(r_1, v_1, r_2, v_2, \dots, r_N, v_N, t) = f_N^{ex}(r, t). \quad (2.11)$$

Using the Eq. (2.11) in Eq. (2.6) and taking the partial derivative of the resultant equation with respect to t yields

$$\frac{\partial f_N^{ex}}{\partial t} = \frac{\partial}{\partial t} \prod_{i=1}^N \delta[r_i - R_i(t)] \delta[v_i - \dot{R}_i(t)], \quad (2.12)$$

$$= - \sum_{i=1}^N \left[R_i \frac{\partial f_N^{ex}}{\partial R_i} + \dot{R}_i \frac{\partial f_N^{ex}}{\partial \dot{R}_i} \right]. \quad (2.13)$$

Using

$$\frac{\partial}{\partial R_i} = \frac{\partial}{\partial r_i}, \quad (2.14)$$

and

$$\frac{\partial}{\partial \dot{R}_i} = \frac{\partial}{\partial v_i} \quad (2.15)$$

in Eq. (2.13), we have

$$\frac{\partial f_N^{ex}}{\partial t} = - \sum_{i=1}^N \left[\dot{R}_i \frac{\partial f_N^{ex}}{\partial r_i} + \dot{R}_i \frac{\partial f_N^{ex}}{\partial \dot{r}_i} \right], \quad (2.16)$$

$$= - \sum_{i=1}^N \left[v_i \frac{\partial f_N^{ex}}{\partial r_i} + \dot{R}_i \frac{\partial f_N^{ex}}{\partial v_i} \right]. \quad (2.17)$$

We can also write Eq. (2.17) as

$$\frac{\partial f_N^{ex}}{\partial t} + \sum_{i=1}^N \left[v_i \frac{\partial f_N^{ex}}{\partial r_i} + \frac{F_i}{m} \frac{\partial f_N^{ex}}{\partial v_i} \right] = 0, \quad (2.18)$$

where $\ddot{R}_i = F_i/m$. The above Eq. (2.18) is responsible for the motion of all the particles present in the plasma.

As we have no information regarding the initial conditions of the system, therefore, it is essential to talk about the system in terms of probability. We presume that at $t=0$, if the distribution function approaches to zero at each point in phase space other than one point (smoother function), it means we are considering an ensemble average over many unknown initial points. Each point in phase space can find a new position after time t that can be determined by studying the dynamics of the system.

2.3 Liouville equation

Consider a 1D analogue of a $6N$ dimensional phase space. The particles which are in small phase space volume $dx dv$ moves from A to B . Due to smallness of $dx dv$, all the particles are subjected to same forces. Thus, all of them moves from one point to the other, and the distribution function is changed to the case in which there are no collisions. During the motion of particles they are unable to cross the surface, i.e. volume of the phase space remains constant. This incompressibility of the phase space volume is recognized as Liouville equation [44].

By denoting the exact distribution function f_N^{ex} by f_N , Eq. (2.18) can be written as

$$\mathbf{L}_N f_N = 0, \quad (2.19)$$

whereas L_N has the following form

$$L_N = \frac{\partial}{\partial t} + \sum_{i=1}^N \left[v_i \frac{\partial}{\partial r_i} + \frac{F_i}{m} \frac{\partial}{\partial v_i} \right]. \quad (2.20)$$

Equation (2.20) is the mathematical form of the Liouville operator. To understand the statistics of a system consists of more than one particles, the Liouville equation is the

beginning with the following mathematical form for a classical system

$$\frac{\partial f_N}{\partial t} + [f_N, H] = 0. \quad (2.21)$$

In the above equation, H is representing the Hamiltonian of the system under consideration.

We define the Poisson bracket, used in Eq. (2.21), as

$$[f_N, H] = \sum_{i=1}^N \left[\frac{\partial f_N}{\partial q_i} \frac{\partial H}{\partial p_i} - \frac{\partial f_N}{\partial p_i} \frac{\partial H}{\partial q_i} \right], \quad (2.22)$$

where p_i and q_i are the conjugate momenta and the generalized coordinates, respectively.

2.4 S-particle distribution function

We can reduce the number of particles to a manageable level from N (very high) to S , such that $S \ll N$. Consequently, the distribution function has the following form

$$f_N(r_1, v_1, r_2, v_2, \dots, r_N, v_N, t) \rightarrow f_S(r_1, v_1, r_2, v_2, \dots, r_S, v_S, t). \quad (2.23)$$

If the number of particles produced is equal to the number of particles destroyed, it means there is no source or sink. Consider the Liouville operator again

$$L_N = \frac{\partial}{\partial t} + \sum_{i=1}^N \left[\dot{r}_i \frac{\partial}{\partial r_i} + a_i \frac{\partial}{\partial v_i} \right], \quad (2.24)$$

which can also be written as

$$L_N = \frac{\partial}{\partial t} + \sum_{i=1}^N \omega_i \frac{\partial}{\partial R_i}. \quad (2.25)$$

By defining

$$r = (X, V), \quad (2.26)$$

and

$$\frac{Dr}{Dt} = (v, a) = \omega, \quad (2.27)$$

Liouville operator turns out to be

$$L_N = \frac{\partial}{\partial t} + \omega \frac{\partial}{\partial t}. \quad (2.28)$$

We can also modify Eq. (2.18) as

$$\frac{\partial f_s}{\partial t} + \sum_{i=1}^S v_i \frac{\partial f_s}{\partial r_i} + \sum_{i=1}^N \frac{1}{m} \left[F_i^{ext} + \sum_{j=1, j \neq i}^S F_{ij} \right] \frac{\partial f_s}{\partial v_i} = 0, \quad (2.29)$$

$$\frac{\partial f_s}{\partial t} + \sum_{i=1}^S v_i \frac{\partial f_s}{\partial r_i} - \sum_{i=1}^S \int d^6 r_{s+1} \frac{F_{s+1}}{m} \frac{\partial f_{s+1}}{\partial v_i} = 0. \quad (2.30)$$

In phase space configuration, to obtain the reduced distribution function we have to integrate the distribution function upon the rest of the variables, i.e. over $S + 1$ to N . Thus, we are left with

$$f_s(r_1, v_1, r_2, v_2, \dots, r_s, v_s, t) = \frac{N!}{(N-S)!} \int f_N \prod_{i=S+1}^N dr_i. \quad (2.31)$$

It means that the total number of possible ways of choosing S particles out of N are $N!/(N-S)!$, thus we have a corresponding normalization constant in Eq. (2.31). There is a specific distribution function corresponding to unit normalization constant. It is possible that we do not know the exact initial point in the phase space. Therefore, f_N^{ex} is changed by f_N , at any later time, the corresponding distribution function $f_N(t)$ can be evaluated by using distribution function at starting point $f(t=0)$. The distribution function f_N is always consistent with the information extracted about the plasma. This extracted microscopic information leads to the ambiguity in f_N as it includes limited (only one or two) space velocity coordinates. The uncertainty in f_N can be taken out by integration over the phase space coordinates. In the following subsection we provide a detailed analysis of the integration over S variables.

2.4.1 BBGKY-Heirarchy

Let us integrate Eq. (2.29) from $S + 1$ to N to obtain S -particle distribution function as follows

$$A_s \int \dots \int \prod_{j=s+1}^N d^6 r_j \left[\frac{\partial f_N}{\partial t} + \sum_{i=1}^N \left(v_i \frac{\partial f_N}{\partial r_i} + a_i \frac{\partial f_N}{\partial v_i} \right) \right] = 0, \quad (2.32)$$

whereas $A_s = N! / (N - S)!$ is the corresponding normalization constant, and let us consider first term

$$I_{a'} = A_s \int \dots \int \prod_{j=s+1}^N d^6 r_j \frac{\partial f_N}{\partial t}, \quad (2.33)$$

$$= \frac{\partial}{\partial t} \left[A_s \int \dots \int \prod_{j=s+1}^N f_N d^6 r_j \right], \quad (2.34)$$

$$= \frac{\partial f_s}{\partial t}. \quad (2.35)$$

The second term of Eq. (2.32) can be written as

$$I_{b'} = A_s \int \dots \int \prod_{j=s+1}^N d^6 r_j \left(\sum_{i=1}^S + \sum_{i=s+1}^N \right) \left[v_i \frac{\partial f_N}{\partial r_i} \right], \quad (2.36)$$

$$= \sum_{i=1}^S \left[v_i \frac{\partial f_s}{\partial r_i} \right] + A_s \sum_{i=s+1}^N \int \dots \int \prod_{j=s+1, j \neq i}^N d^6 r_j \int v_i d^3 v_i \int \frac{\partial f_N}{\partial r_i} d^3 r_i, \quad (2.37)$$

$$= \sum_i^S \frac{\partial f_s}{\partial r_i}. \quad (2.38)$$

In the same way we have

$$I_{c'} = A_s \int \dots \int \prod_{j=s+1}^N d^6 r_j \sum_{i=1}^N \frac{F_i}{m} \frac{\partial f_N}{\partial v_i}, \quad (2.39)$$

$$= A_s \int \dots \int \prod_{j=s+1}^N d^6 r_j \frac{F_i}{m} \frac{\partial f_N}{\partial v_i} + A_s \sum_{i=s+1}^N \int \dots \int \prod_{j=s+1, j \neq i}^N d^6 r_j \int d^3 r_i \int \frac{d^3 v_i}{m} \left[ZeE(r,t)Ze(v \times B) + mg(r,t) \right] \frac{\partial f_N}{\partial v_i}. \quad (2.40)$$

Next, we consider the last term and applying Gauss's theorem to write

$$I_{d'} = \int d^3 v_i a(r, v, t) \frac{\partial f_N}{\partial v_i}, \quad (2.41)$$

$$= \int d^3 v_i \left[\frac{\partial (a_i f_N)}{\partial v_i} - f_N \frac{\partial a_i}{\partial v_i} \right], \quad (2.42)$$

$$\oint_{v \rightarrow \infty} d^3 v_i (a_i f_N) = 0. \quad (2.43)$$

Here we have used the condition that f_N vanishes at the boundaries of phase space Γ . Thus, we have Eq. (2.32) in the following form

$$\frac{\partial f_s}{\partial t} + \sum_{i=1}^S v_i \frac{\partial f_s}{\partial r_i} + A_s \int \dots \int \prod_{i=s+1}^N d^6 r_j \frac{F_i}{m} \frac{\partial f_N}{\partial v_i} = 0. \quad (2.44)$$

Now we decompose the force F_i into two parts, the force exerted due to the externally applied fields, and the second is due to the all internal interactions occurring between the plasma particles present in the system, i.e.

$$F_i = F_i^{ext} + F_i^{int}, \quad (2.45)$$

$$= F_i^{ext} + \sum_{j=1, j \neq i}^N F_{ij}. \quad (2.46)$$

While

$$F_i^{ext} = F_i^{ext}(r_i, t), \quad (2.47)$$

and

$$F_i^{int} = F_i^{int}(r_1, r_2, r_3, \dots, r_N). \quad (2.48)$$

The external force part from Eq. (2.47) yields

$$I_{el} = \sum_{i=1}^S A_s \int \dots \int \prod_{j=s+1}^N d^6 r_j \frac{F_i^{ext}(r_i, t)}{m} \frac{\partial f_N}{\partial v_i}(r_1, \dots, r_i, \dots, r_s, r_{s+1}, \dots, r_N), \quad (2.49)$$

$$= \frac{1}{m} \sum_{i=1}^S F_i^{ext} \frac{\partial}{\partial v_i} \int_{N-S} \dots \int \prod_{j=s+1}^N f_N d^6 r_j, \quad (2.50)$$

$$= \sum_{i=1}^S \frac{F_i^{ext}}{m} \frac{\partial f_N}{\partial v_i}. \quad (2.51)$$

Similarly, one can find

$$I_{f'} = \sum_{i=1}^S A_s \int \dots \int \prod_{j=s+1}^N \frac{1}{m} d^6 r_j \left[\sum_{k=1}^s F_{ik}(v_i, v_k) + \sum_{k=s+1}^N F_{ik}(r_i, v_k) \right] \frac{\partial f_N}{\partial v_i}. \quad (2.52)$$

Hence, Eq. (2.52) can be written as

$$I_{f'} = I_{f_1'} + I_{f_2'}, \quad (2.53)$$

where

$$I_{f_1'} = \frac{A_s}{m} \sum_{i=1}^S \sum_{k=1}^s F_{ik} \frac{\partial}{\partial v_i} \int_{N-S} \dots \int \prod_{j=s+1}^N f_N d^6 r_j, \quad (2.54)$$

$$= \sum_{i=1}^S \sum_{j=1}^s \frac{F_{ij}}{m} \frac{\partial f_s}{\partial v_i}, \quad (2.55)$$

and

$$I_{f_2'} = \frac{A_s}{m} \sum_{i=1}^S \sum_{k=s+1}^S \int F_{ik} d^6 r_k \frac{\partial}{\partial v_i} \int \dots \int \prod_{j=s+1, j \neq k}^N f_N d^6 r_j, \quad (2.56)$$

$$= \frac{A_s}{m} \sum_{i=1}^S \sum_{k=s+1}^S \int F_{ik}(r_i, r_k) d^6 r_k \frac{\partial}{\partial v_i} f_{s+1}(r_1, \dots, r_s, \dots, r_k, t). \quad (2.57)$$

This integral will be same for any k such that

$$S+1 \leq k \leq N,$$

which means that there are $N - S$ possible ways for $k = N - S$ integrals. Therefore, we have k for $S + 1$ times and can easily remove the second summation in $I_{f_2'}$ to write

$$I_{f_2'} = \frac{A_s}{mA_{s+1}} \sum_{i=1}^S (N - S) \int F_{i,s+1} d^6 r_{s+1} \frac{\partial}{\partial v_i} f_{s+1}(r_1, \dots, r_s, \dots, r_{s+1}, t). \quad (2.58)$$

Since we have the normalization constant given by

$$A_s = \frac{N!}{(N - S)!},$$

which provides the following expression

$$\frac{A_s(N - S)}{A_{s+1}} = \frac{(N - S - 1)!(N - S)}{(N - S)!} = 1.$$

Thus, the conclusive expression for f_s comes out to be

$$\frac{\partial f_s}{\partial t} + \sum_{i=1}^S v_i \frac{\partial f_s}{\partial t} + \sum_{i=1}^S \frac{1}{m} \left[F_i^{ext} + \sum_{j=1, j \neq i}^S F_{ij} \right] \frac{\partial f_s}{\partial v_i} = - \sum_{i=1}^S \int d^6 r_{s+1} \frac{F_{i,s+1}}{m} \frac{\partial f_s}{\partial v_i}. \quad (2.59)$$

The interaction term is shown on the right hand side of the above Eq. (2.59). We need a physical approximation in the above equation because f_s contain f_{s+1} terms. In other words we can say that to get a solution of f_s , we need a prior solution of f_{s+1} . This is known as the Bogolyubov, Born Green, Kirkwood, and Yvon (BBGKY) hierarchy [45].

We have achieved no simplification in the sense that we need f_{s+1} to get the result of f_s . To get rid of this complexity, we made some approximation, e.g. cluster expansion. In this equation the function f_2, \dots, f_s are used, leaving a single particle distribution function f_1 . It means that we remove $S - 1$ equations out of S equations. The S -particle Liouville equation will be read as following

$$\frac{\partial f_1}{\partial t} + v_1 \frac{\partial f_1}{\partial r_i} + \left[\frac{F_i^{ext}}{m} \frac{\partial f_1}{\partial v_1} \right] = - \int d^2 r_2 \frac{F_{12}}{m} \frac{\partial f_1}{\partial v_1}. \quad (2.60)$$

Now, let us learn about the approximation, namely, a cluster expansion, to deal with BBGKY hierarchy.

2.5 Cluster expansion

The distribution function $f_1 = f_1(r_1, v_1, t)$ can be used to evaluate the probability of finding the particle 1 at position r_1 with velocity v_1 at any time t . Similarly, a two-particle distribution function $f_2 = f_2(r_1, v_1, r_2, v_2, t)$ is employed to obtain the probability of finding the particle 1 at position r_1 with velocity v_1 at any time t and at the same time particle 2 at position r_2 with velocity v_2 . This two-particle distribution function gives information only about the two particles. Consider the two functions f_1 and f_2 , a third function f_3 can be defined by using these two functions. In this new function, we may introduce an expansion that is known as cluster expansion. As $f_1(r_1, v_1, t)$ is the distribution function of a single particle, $f_2(r_1, v_1, r_2, v_2, t)$ is the two particle distribution function, and $F_{12}(r_1, v_1, r_2, v_2, t)$ is the force exerted on particle 1 by the particle 2.

Let us introduce some new notations for mathematical convenience

$$f_1(r_1, v_1, t) = f_1(1), \quad (2.61)$$

and

$$f_2(r_1, v_1, r_2, v_2, t) = f_2(1, 2). \quad (2.62)$$

In terms of the cluster expansion, we can write the relation between two particle distribution function in terms of one particle distribution function as

$$f_2(1, 2) = f_1(r_1, v_1, t)f_1(r_2, v_2, t) + p(r_1, v_1, r_2, v_2, t), \quad (2.63)$$

and, in more simplified form

$$f_2(1, 2) = f_1 f_2 + p(1, 2), \quad (2.64)$$

where $p(1, 2)$ is a pair correlation function. Similarly, a three-particle distribution function in the form of cluster expansion

$$\begin{aligned}
f_3(r_1, v_1, r_2, v_2, r_3, v_3, t) &= f(r_1, v_1, t)f(r_2, v_2, t)f(r_3, v_3, t) + f(r_1, v_1, t)p(r_2, v_2, r_3, v_3, t) + \\
&f(r_2, v_2, t)p(r_1, v_1, r_3, v_3, t) + f(r_3, v_3, t)p(r_1, v_1, r_2, v_2, t) + \\
&T(r_1, v_1, r_2, v_2, r_3, v_3, t).
\end{aligned}
\tag{2.65}$$

Equation (2.65) can also be written in a more compact form as

$$f_3(1, 2, 3) = f(1)f(2)f(3) + f(1)f(2, 3) + f(2)f(1, 3) + f(3)f(1, 2) + T(1, 2, 3). \tag{2.66}$$

The basic idea of the cluster expansion is that the probability to find the electron can be obtained by multiplying $f(1)$ and $f(2)$. If the particle 1 and particle 2 are not dependent on each other. Thus, $p(1, 2)$ function be viewed as the variation between the function f_2 and $f(1)f(2)$ which employs that the particle 1 and 2 are interacting and dependent. Therefore, we say that the function $f(1, 2)$ and $p(1, 2)$ is a pair correlation and likewise $T(1, 2, 3)$ is a tri-correlation function.

For the special case of two particles to be at the same position, i.e.

$$|r_1 - r_2| = 0,$$

we must have

$$f_2(1, 2) = 0. \tag{2.67}$$

And thus for the above-mentioned case one finds

$$p(1, 2) = -f(1)f(2), \tag{2.68}$$

where the reason for a negative sign is that the both f_1 and f_2 are positive. Next, we consider the case in which the distance between the two particles is very large, i.e. they are

infinite apart, namely

$$|r_1 - r_2| = \infty$$

then $p(1,2) = 0$. It means $f_2(1,2) = f_1 f_2$. In this case, the particles are not correlated by any means.

By using Eqs. (2.61) and (2.64) in Eq. (2.60), we find

$$\frac{\partial f(1)}{\partial t} + v_1 \frac{\partial f(1)}{\partial r_1} + \left[a_1^{ext} \frac{\partial f(1)}{\partial v_1} \right] = - \int d^6 r_2 a_{12} \frac{\partial}{\partial v} \left[f(1) f(2) + p(1,2) \right], \quad (2.69)$$

which can also be written as

$$\frac{\partial f(1)}{\partial t} + v_1 \frac{\partial f(1)}{\partial r_1} + \frac{1}{m} \left[F(1)^{ext} + \int d^6 r_2 f(2) F_{12}(1,2) \right] \frac{\partial f(1)}{\partial v_1} = - \int d^6 r_2 a_{12} \frac{\partial p(1,2)}{\partial v_1}, \quad (2.70)$$

where external force is denoted by $F(1)^{ext}$ and the integral $\int d^6 r_2 f(2) F_{12}(1,2)$ is the self-consistent force. The sum of external force and the self-consistent force is known as the macroscopic force, which corresponds to the acceleration as given by

$$a^{mac} = \frac{1}{m} \left[F(1)^{ext} + \int d^6 r_2 f(2) F_{12}(1,2) \right]. \quad (2.71)$$

Here we average over v and r hence the final form of the generalized kinetic equation reads

$$\frac{\partial f(1)}{\partial t} + v_1 \frac{\partial f(1)}{\partial r_1} + a^{mac} \frac{\partial f(1)}{\partial v_1} = - \int d^6 r_2 a_{12} \frac{\partial p(1,2)}{\partial v_1}. \quad (2.72)$$

The above Eq. (2.72) can be understood in the way that when electric force is experienced by particle 1 due to particle 2, for computing this force we assume that the particles are not correlated. The correlation of particle 1 with particle 2 is not considered when we are taking the average over entire velocities and positions of particle 2 and vice versa. This result deduced from the right hand side of the above equation. The right hand side is actually the part of self-consistent field, contributed by the particles.

We have $a = F/m$ which includes the affect of all the fields and external forces. The

function $f(r, v, t)$ is the one particle distribution function that represents one of the particles out of many particle system of specific nature. Therefore, the information obtained from this distribution function is not helpful to distinguish the kinetic behavior of a single particle.

However, we do not specify which single particle it is. Thus, actually $f(r, v, t)$ is the one special distribution function such that when integrated over velocity, it provides the number density of the corresponding species.

Chapter 3

Slowing down by small angle Coulomb collisions

Let us consider the case in which $n(\mathbf{r}, \mathbf{v}, t)d^3rd^3v$ is the number of particles anticipated at time t in d^3r about \mathbf{r} and in d^3v about \mathbf{v} . The transport equation for a single-particle's density distribution function $n(\mathbf{r}, \mathbf{v}, t)$ can be written as

$$\frac{\partial n(\mathbf{r}, \mathbf{v}, t)}{\partial t} + \mathbf{v} \cdot \Delta_{\mathbf{r}} n + Ze/m[\mathbf{E} + \mathbf{v} \times \mathbf{B}] \cdot \Delta_{\mathbf{v}} n = \left(\frac{\partial n}{\partial t} \right)_{c(\text{collisions})} + \left(\frac{\partial n}{\partial t} \right)_{s(\text{sources or sinks})} \quad (3.1)$$

with the very well known relation

$$\int_{-\infty}^{+\infty} d^3v n(\mathbf{r}, \mathbf{v}, t) = n(\mathbf{r}, t), \quad (3.2)$$

which represents the density of particles at \mathbf{r} . In order to determine a source/sink term by outside sources or the kinematics of reactions which deliver the strength density $S(\mathbf{r}, \mathbf{v}, t)$ of source/sink, one is needed to specify the collision term via theoretical means utilizing valid approximations or statistical approaches.

If $\left(\frac{\partial n}{\partial t} \right)_c = 0$, it means there are no collisions or we have a “collision free” case. in other words we say that there is no change in n due to collisions, but changes are taking

place due to internal and external fields. As a result we get Boltzmann distribution function.

$$\left(\frac{\partial n}{\partial t}\right)_c = 0 \Rightarrow \text{Vlasov equation}$$

As the collisions are taking place in the plasma, the distribution function will change. To take care of these collisions we introduce a new function $P(\mathbf{r}, \mathbf{v}, \Delta\mathbf{v})$. This newly introduced function provides the probability of a particle moving at position \mathbf{r} with velocity \mathbf{v} to alter its velocity due to collisions from \mathbf{v} to $\mathbf{v} + \Delta\mathbf{v}$ in an interval of time Δt . We must know that $P(0) \neq P(t)$. It means that the probability for change in velocity due to collision does not depend on what happens before the collision. Those processes for which the above mentioned condition holds are known as Markov processes. Obviously, the normalization condition

$$\int_{-\infty}^{+\infty} d^3\Delta\mathbf{v}P(\mathbf{r}, \mathbf{v}, \Delta\mathbf{v}) = 1, \quad (3.3)$$

holds.

Now by using $P(\mathbf{r}, \mathbf{v}, \Delta\mathbf{v})$ we can write the distribution function $n(\mathbf{r}, \mathbf{v}, t)$ with the help of distribution function before collision as follows

$$n(\mathbf{r}, \mathbf{v}, t) = \int_{-\infty}^{+\infty} d^3\Delta\mathbf{v}P(\mathbf{r}, \mathbf{v} - \Delta\mathbf{v}, \Delta\mathbf{v})n(\mathbf{r}, \mathbf{v} - \Delta\mathbf{v}, t - \Delta t), \quad (3.4)$$

valid for $\Delta t \rightarrow 0$ that means $\mathbf{r} \approx \text{constant}$.

We suppose that the major effects of collision are because of Coulomb interaction. In Coulomb interactions small angle scatterings dominates the large angle scattering events by a factor of 100. The change in velocity $\Delta\mathbf{v}$ can be considered small enough for small Δt . Therefore the above expression can be expanded via a Taylor series for small values of $\Delta\mathbf{v}$

and Δt to have

$$\begin{aligned}
n(\mathbf{r}, \mathbf{v}, t) = & \int_{-\infty}^{+\infty} d^3 \Delta \mathbf{v} \left\{ n(\mathbf{r}, \mathbf{v}, t) P(\mathbf{r}, \mathbf{v}, \Delta \mathbf{v}) - \Delta t P(\mathbf{r}, \mathbf{v}, \Delta \mathbf{v}) \frac{\partial n(\mathbf{r}, \mathbf{v}, t)}{\partial t} - \Delta \mathbf{v} \cdot \nabla_{\mathbf{v}} [n(\mathbf{r}, \mathbf{v}, t) P(\mathbf{r}, \mathbf{v}, \Delta \mathbf{v})] + \right. \\
& \frac{1}{2} \sum_m \sum_n \Delta v_m \Delta v_n \frac{\partial^2}{\partial v_m \partial v_n} [n(\mathbf{r}, \mathbf{v}, t) P(\mathbf{r}, \mathbf{v}, \Delta \mathbf{v})] + \\
& \left. O(\Delta t \Delta t) + O(\Delta t \Delta v) + O(\Delta t \Delta t \Delta v) + O(\Delta t \Delta v \Delta v) + \dots \right\}.
\end{aligned} \tag{3.5}$$

We realize that the number density distribution function is independent of $\Delta \mathbf{v}$ so the series is terminated after order $O(\Delta t \Delta v \Delta v)$. By the use of normalization condition $P(\mathbf{r}, \mathbf{v}, \Delta \mathbf{v}) = 1$, we can see that the LHS term gets cancel with the first term on the RHS and we left with

$$\begin{aligned}
\Delta t \frac{\partial n(\mathbf{r}, \mathbf{v}, t)}{\partial t} = & - \sum_m \frac{\partial}{\partial v_m} n(\mathbf{r}, \mathbf{v}, t) \int_{-\infty}^{+\infty} d^3(\Delta v) \Delta v_m P(\mathbf{r}, \mathbf{v}, \Delta \mathbf{v}) \\
& \frac{1}{2} \sum_m \sum_n \Delta v_m \Delta v_n \frac{\partial^2}{\partial v_m \partial v_n} n(\mathbf{r}, \mathbf{v}, t) \int_{-\infty}^{+\infty} d^3(\Delta v) \Delta v_m \Delta v_n P(\mathbf{r}, \mathbf{v}, \Delta \mathbf{v}).
\end{aligned} \tag{3.6}$$

As it is presumed that the changes occur due to collision will be incorporated only, the changes occur in the number density distribution function with respect to time is certainly the term $\left(\frac{\partial n(\mathbf{r}, \mathbf{v}, t)}{\partial t} \right)_c$ as calculated above and we are going to give it the superscript *FP* for recognition as Fokker-Planck collision term. Furthermore, it can be understood that the above integrals are actually the mean values of $\langle \Delta \mathbf{v} \rangle$ and $\langle \Delta v_m \Delta v_n \rangle$.

By Fokker-Planck equation, the kinetics of charged particle is described as, for a specific particle species *i*

$$\begin{aligned}
\left(\frac{\partial n_i(\mathbf{r}, \mathbf{v}_i, t)}{\partial t} \right)_c^{FP} = & - \sum_m \frac{\partial}{\partial v_{i,m}} \left\{ n_i(\mathbf{r}, \mathbf{v}_i, t) \frac{\langle \Delta v_{i,m} \rangle}{\Delta t} \right\} + \frac{1}{2} \\
& \sum_m \sum_n \frac{\partial^2}{\partial v_{i,m} \partial v_{i,n}} \left\{ n_i(\mathbf{r}, \mathbf{v}_i, t) \frac{\langle \Delta v_{i,m} \Delta v_{i,n} \rangle}{\Delta t} \right\},
\end{aligned} \tag{3.7}$$

where the term $\frac{\langle \Delta v_{i,m} \rangle}{\Delta t}$ is the mean rate of collisional vibration in the single velocity. This is also known as dynamical friction or drag in the velocity space. The term $\frac{\langle \Delta v_{i,m} \Delta v_{i,n} \rangle}{\Delta t}$ gives the collisional change of the distribution of the velocity and is the so-called velocity

diffusion.

The average value of any arbitrary function Z of Δv_i can be written as following integral

$$\langle Z(\Delta v_i) \rangle = \int_{-\infty}^{+\infty} Z(\Delta v_i) P(\mathbf{r}, \mathbf{v}_i; \Delta v_i) d^3 v_i = \int_{4\pi} Z(\Omega) \omega(\mathbf{r}, \mathbf{v}_i; \Omega) d^2 \Omega, \quad (3.8)$$

where $\omega(\mathbf{r}, \mathbf{v}_i; \Omega)$ gives the probability of changing the relative velocity by the solid angle Ω . The relative velocity v_r of a particle i moving with velocity v_i is changed due to its elastic collision with particles j having all possible velocities and is at position represented by r . The new relative velocity v_r' corresponds to the collisional change of angle $\Omega + d^2 \Omega$ with respect to the initial relative velocity v_r . In order to find $\omega(\mathbf{r}, \mathbf{v}_i; \Omega)$, let us integrate over all scattering reactions which involve particle i with velocity v_i and particles j of all velocities, which bring about a unique scattering angle $\Omega(v_r', v_r)$:

$$\omega(\mathbf{r}, \mathbf{v}_i; \Omega) = \Delta t \int_{-\infty}^{+\infty} \sigma_{ij}(|v_i - v_j|, \Omega) |v_i - v_j| n_j(\mathbf{r}, \mathbf{v}_j, t) d^3 v_j. \quad (3.9)$$

The mean rate of change of single velocity, in other words the dynamical friction, can be calculated as

$$\frac{\langle \Delta v_i \rangle}{\Delta t} = \frac{1}{\Delta t} \int_{4\pi} \Delta v_i \omega(\mathbf{r}, \mathbf{v}_i; \Omega) d^2 \Omega = \int_{-\infty}^{+\infty} d^3 v_j \int_{4\pi} d^2 \Omega \Delta v_i n_j(\mathbf{r}, \mathbf{v}_j, t) \sigma_{ij}(v_r, \Omega) v_r, \quad (3.10)$$

with the following relation satisfied

$$\Delta v_i = \frac{m_r}{m_i} \Delta v_i = \frac{m_r}{m_i} v_r \begin{pmatrix} -2 \sin^2(\theta) \\ \sin(\theta) \cos(\epsilon) \\ \sin(\theta) \sin(\epsilon) \end{pmatrix}. \quad (3.11)$$

The above value of Δv_i is according to the scheme shown in Fig. (3.1). The function $\sigma_{ij}(v_r, \Omega)$ in Eq. (3.10) represents the Coulomb's reaction cross section and is given by

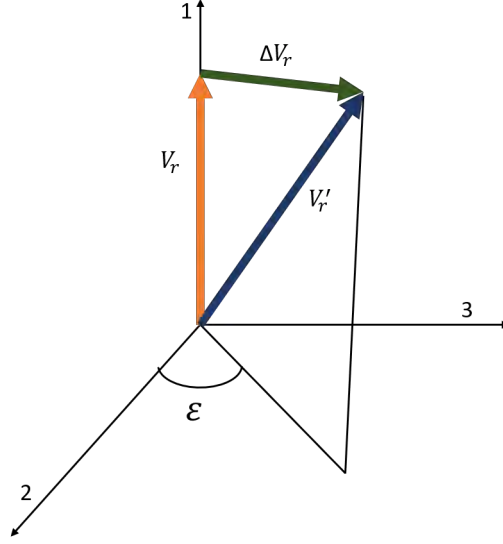


Figure 3.1: Scheme for $\Delta\mathbf{v}_i$ in terms of relative velocities v_r and v'_r .

[46]

$$\sigma_{ij}(v_r, \Omega) = \sigma_{ij}^{Cou.}(v_r, \Omega) = \frac{1}{2\pi} \sigma_{ij}^{Cou.}(v_r, \theta_{(CM)}) = \frac{(Z_i Z_j e^2 / 4\pi\epsilon_0)^2}{8\pi m_r^2 v_r^4} \sin^{-4}\left(\frac{\theta}{2}\right). \quad (3.12)$$

After some straightforward calculations, we find the following

$$\begin{aligned} \frac{\langle \Delta v_i \rangle}{\Delta t} &\approx \left\langle \frac{\Delta v_i}{\Delta t} \right\rangle = \frac{(Z_i Z_j e^2)^2}{(4\pi\epsilon_0)^2 8\pi m_r^2} \int_{-\infty}^{+\infty} d^3 v_j n_j(\mathbf{r}, \mathbf{v}_j, t) \frac{v_r}{v_r^4} \int_0^\pi d\theta \frac{\sin(\theta)}{\sin^4(\theta/2)} \\ &\int_0^{2\pi} d\epsilon \frac{m_r}{m_i} v_r \begin{pmatrix} -2 \sin^2(\theta) \\ \sin(\theta) \cos(\epsilon) \\ \sin(\theta) \sin(\epsilon) \end{pmatrix} \\ &= \frac{(Z_i Z_j e^2)^2}{(4\pi\epsilon_0)^2 8\pi m_r m_i} \int_{-\infty}^{+\infty} d^3 v_j n_j(\mathbf{r}, \mathbf{v}_j, t) \frac{1}{v_r^2} \int_0^\pi d\theta \frac{\sin(\theta)}{\sin^4(\theta/2)} \\ &\int_0^{2\pi} d\epsilon \frac{m_r}{m_i} v_r \begin{pmatrix} -4\pi \sin^2(\theta) \\ 0 \\ 0 \end{pmatrix} \\ &= -\frac{(Z_i Z_j e^2)^2}{(4\pi\epsilon_0)^2 2m_r m_i} \int_{-\infty}^{+\infty} d^3 v_j n_j(\mathbf{r}, \mathbf{v}_j, t) \frac{1}{v_r^2} \int_0^\pi d\theta \frac{\sin(\theta)}{\sin^2(\theta/2)} \mathbf{e} \cdot \mathbf{1}, \end{aligned} \quad (3.13)$$

where $\mathbf{e}_1 = \frac{\mathbf{v}_r}{v_r}$ is the corresponding unit vector.

To get rid of the divergence of the integral $\int_0^\pi d\theta \frac{\sin(\theta)}{\sin^2(\theta/2)} = 4 \int_0^{\pi/2} \cot(\theta/2) d(\theta/2)$, i.e., not responsible for insignificant Coulomb collisions but taking into account most significant one. The lower limit of the integral is actually a cut off at a scattering angle which is minimum and effective. Its value is [47]

$$\theta_{min}/2 = \tan^{-1} \left(\frac{Z_i Z_j e^2}{4\pi\epsilon_0 m_r v_r^2} \cdot \frac{1}{b} \right). \quad (3.14)$$

Here b is the corresponding impact parameter and is given as

$$b \approx \lambda_D = \sqrt{\frac{\epsilon_0 k T}{n e^2}}, \quad (3.15)$$

the above relation taken into account the chance of interaction outside this impact parameter's range, which is minimum due to charge shielding. This is adequate for $\lambda_D \gg \lambda_{Broglie}$, otherwise a quantum-mechanical treatment is necessary. Therefore, we have

$$\theta_{min}/2 = \tan^{-1} \left(\frac{Z_i Z_j e^2}{4\pi\epsilon_0 m_r v_r^2} \cdot \frac{1}{\lambda_D} \right). \quad (3.16)$$

We may define

$$\begin{aligned} \int_{\theta_{min}/2}^{\pi/2} \cot(\theta/2) d(\theta/2) &= \ln\{\sin(x)\} \Big|_{\theta_{min}/2}^{\pi/2} = -\ln\{\sin(\theta_{min}/2)\} \\ &=: \ln(\Lambda_{ij}) =: \text{CoulombLogrithmus}, \end{aligned} \quad (3.17)$$

to get the final result of $\left\langle \frac{\Delta v_i}{\Delta t} \right\rangle$, one can write

$$\left\langle \frac{\Delta v_i}{\Delta t} \right\rangle = -\frac{2(Z_i Z_j e^2)^2}{(4\pi\epsilon_0)^2 m_r m_i} \int_{-\infty}^{+\infty} d^3 v_j \ln \Lambda_{ij} \frac{\mathbf{v}_r}{v_r^3} n_j(\mathbf{r}, \mathbf{v}_j, t). \quad (3.18)$$

Upon using the same analogy we may write for diffusion term

$$\left\langle \frac{\Delta v_{i,m} \Delta v_{i,n}}{\Delta t} \right\rangle = +\frac{2(Z_i Z_j e^2)^2}{(4\pi\epsilon_0)^2 m_i^2} \int_{-\infty}^{+\infty} d^3 v_j \ln \Lambda_{ij} \frac{\partial^2 v_r}{\partial v_{i,m} \partial v_{i,n}} \frac{\mathbf{v}_r}{v_r^3} n_j(\mathbf{r}, \mathbf{v}_j, t). \quad (3.19)$$

Using Eqs. (3.18) and (3.19) into the Fokker-Planck collision term and introducing the latter into the transport equation gives us the Fokker-Planck equation.

Now we are going to find the energy variation of a highly energetic particle slowing down due to collisions with the particles of a thermal background plasma, for that we find the mean rate of energy transfer in Coulomb collisions, $\left\langle \frac{\Delta E_i}{\Delta t} \right\rangle$. Let us first calculate

$$\begin{aligned}\Delta E_i &= \frac{m_i}{2} \left[(\mathbf{v}_i + \Delta \mathbf{v}_i)^2 - \mathbf{v}_i^2 \right] \\ &= \frac{m_i}{2} \left[(\mathbf{v}_i^2 + 2\mathbf{v}_i \cdot \Delta \mathbf{v}_i) + (\Delta \mathbf{v}_i)^2 - \mathbf{v}_i^2 \right], \\ &= \frac{m_i}{2} \left[2\mathbf{v}_i \cdot \Delta \mathbf{v}_i + \left(\frac{m_r}{m_i} \Delta \mathbf{v}_r \right)^2 \right]\end{aligned}\quad (3.20)$$

where

$$2\mathbf{v}_i \cdot \Delta \mathbf{v}_i = 2(\mathbf{v}_{CM} \frac{m_r}{m_i} \Delta \mathbf{v}_r) \cdot \frac{m_r}{m_i} \Delta \mathbf{v}_r = 2 \frac{m_r}{m_i} \left[\mathbf{v}_{CM} \cdot \Delta \mathbf{v}_r + \frac{m_r}{m_i} \mathbf{v}_r \cdot \Delta \mathbf{v}_r \right]. \quad (3.21)$$

As, for an elastic collision, the magnitude of the relative velocity remains same, thus we can use the following relation

$$\Delta(\mathbf{v}_r)^2 = 0 = \left[(\mathbf{v}_r + \Delta \mathbf{v}_r)^2 - \mathbf{v}_r^2 \right] = \left[2\mathbf{v}_r \cdot \Delta \mathbf{v}_r + (\Delta \mathbf{v}_r)^2 \right], \quad (3.22)$$

to write

$$(\Delta \mathbf{v}_r)^2 = -2\mathbf{v}_r \cdot \Delta \mathbf{v}_r. \quad (3.23)$$

By using these expressions in Eq. (3.20)

$$\Delta E_i = m_r \mathbf{v}_{CM} \cdot \Delta \mathbf{v}_r, \quad (3.24)$$

is easily found with constant value for \mathbf{v}_{CM} .

By using our earlier definitions, we can write

$$\begin{aligned}
\left\langle \frac{\Delta E_i}{\Delta t} \right\rangle &= \int_{-\infty}^{+\infty} d^3 v_j \int_{4\pi} d^2 \Omega n_j(\mathbf{r}, \mathbf{v}_j, t) \sigma_{ij}(v_r, \Omega) v_r \Delta E_i(\Delta \mathbf{v}_r(\Omega)) \\
&= \int_{-\infty}^{+\infty} d^3 v_j \int_{0 \rightarrow \theta_{min}}^{\pi} d\theta \sin(\theta) \int_0^{2\pi} d\varepsilon n_j(\mathbf{r}, \mathbf{v}_j, t) v_r \frac{1}{2\pi} \sigma_{ij}^{Coul.}(v_r, \theta) \times m_r \\
&\quad \left\{ \mathbf{v}_{CM}(-2v_r \sin^2(\theta/2)) \cdot \frac{\mathbf{v}_r}{v_r} + v_r \left[(\mathbf{v}_{CM} \cdot \mathbf{e}_2) \cos(\varepsilon) + (\mathbf{v}_{CM} \cdot \mathbf{e}_3) \sin(\varepsilon) \right] \sin(\theta) \right\},
\end{aligned} \tag{3.25}$$

where the unit vectors \mathbf{e}_2 and \mathbf{e}_3 , used above, are perpendicular to $\mathbf{e}_1 = \frac{\mathbf{v}_r}{v_r}$. The integration of the terms containing $\cos(\varepsilon)$ and $\sin(\varepsilon)$ vanishes over the full period of ε . Therefore, we have

$$\int_0^{2\pi} d\varepsilon \Delta E_i = -4\pi m_r (\mathbf{v}_{CM} \cdot \mathbf{v}_r) \sin^2(\theta/2), \tag{3.26}$$

to write a final expression as

$$\begin{aligned}
\left\langle \frac{\Delta E_i}{\Delta t} \right\rangle_{i \rightarrow j} &= -\frac{(Z_i Z_j e^2)^2}{(4\pi \varepsilon_0)^2 2m_r} \int_{-\infty}^{+\infty} d^3 v_j n_j(\mathbf{r}, \mathbf{v}_j, t) (\mathbf{v}_{CM} \cdot \mathbf{v}_r) \frac{v_r}{v_r^4} \int_{0 \rightarrow \theta_{min}}^{\pi} d\theta \sin(\theta) \frac{\sin^2(\theta/2)}{\sin^4(\theta/2)}, \\
&= -\frac{2(Z_i Z_j e^2)^2}{(4\pi \varepsilon_0)^2 m_r} \int_{-\infty}^{+\infty} d^3 v_j n_j(\mathbf{r}, \mathbf{v}_j, t) \ln \Lambda_{ij} \frac{(\mathbf{v}_{CM} \cdot \mathbf{v}_r)}{v_r}.
\end{aligned} \tag{3.27}$$

Above relation provides the mean rate of energy transfer from particle i to j in Coulomb collisions. As the dependence of $\ln \Lambda$ on v_r is weak (of 2^{nd} order), therefore the Coulomb logarithm can be placed in front of the integral. If the constituents of plasma, with which the particle- i collides, are more than one, then the mean energy loss or the stopping power is obtained by superposition over all such particles, namely

$$\left\langle \frac{\Delta E_i}{\Delta t} \right\rangle = \sum_j \left\langle \frac{\Delta E_i}{\Delta t} \right\rangle_{i \rightarrow j}. \tag{3.28}$$

The mean energy loss is also given the name of gain rate by collisions [46].

The above expression to find the stopping power is applicable for continuous slowing down. The continuous slowing down occurs if the leading deceleration tool are small angle Coulomb collisions, i.e., small angle collisions are taken to be more frequent.

If the velocity distribution is isotropic of the particles j , the Fokker-Planck equation can be re-written in the energy variable as

$$\left(\frac{\partial n_i(\mathbf{r}, E_i, t)}{\partial t}\right)_c^{FP} = \frac{\partial}{\partial t} \left\{ \left\langle \frac{\Delta E_i}{\Delta t} \right\rangle n_i(\mathbf{r}, E_i, t) \right\} + \frac{1}{2} \frac{\partial^2}{\partial E_i^2} \left(D_i(\mathbf{r}, E_i) n_i(\mathbf{r}, E_i, t) \right), \quad (3.29)$$

where D_i is the energy diffusion rate and is given by

$$D_i \approx \left\langle \left(\frac{\Delta E_i}{\Delta t} \right)^2 \right\rangle - \left\langle \frac{\Delta E_i}{\Delta t} \right\rangle^2. \quad (3.30)$$

We know that the derivation of the Fokker-Planck equation is based on the assumption of small energy transfer collisions. These collisions are certainly the scattering events which occurs more frequently in fusion plasmas. Undoubtedly, this depiction of energy transition cannot be applied to collisions with discrete, large energy transfer. Such events require discrete analysis of energy transitions as provided by binary collision model of the Boltzmann description [48].

3.1 Slowing down of fast ions

Let us define a function given in the form of integral as

$$G_j(x_j) = \sqrt{\frac{m_j}{2kT_j}} \int_{-\infty}^{+\infty} d^3 v_j f_j(\mathbf{v}_j) |\mathbf{v}_b - \mathbf{v}_j|, \quad (3.31)$$

with $n_j(\mathbf{r}) f_j(\mathbf{j}) = n_j(\mathbf{r}, \mathbf{v}_j)$ and

$$x_j = \frac{v_b}{v_{j,thermal}} = \frac{v_b}{\sqrt{2kT_j/m_j}}. \quad (3.32)$$

Upon introducing the function define above in Eqs. (3.18) and (3.19), we are able to get an expansion of the Fokker-Planck collision term. These collision are taking place among

a test particle b (i.e. beam injected) with the constituents j of background plasma, whereas j is denoting electrons, bulk ions etc. Thus, we consider beam-plasma system with corresponding equation as given by

$$\begin{aligned} \left(\frac{\partial n_b(\mathbf{r}, \mathbf{v}_b, t)}{\partial t} \right) = \sum_j \left(\frac{Z_b Z_j e^2}{4\pi\epsilon_0} \right)^2 \frac{2\pi n_j(\mathbf{r}) \ln \Lambda_{b,j}}{m_b^2} \frac{\partial}{\partial v_{b,m}} \left[\frac{\partial n_b}{\partial v_{b,n}} \left(\frac{\partial^2 v_b}{\partial v_{b,m} \partial v_{b,n}} G I_j(x_j) + \right. \right. \\ \left. \left. \frac{v_{b,m} v_{b,n}}{v_b^3} x_j G II_j(x_j) \right) + 2 \frac{m_b}{m_j} n_b(\mathbf{r}, \mathbf{v}, t) \frac{v_{b,m}}{v_b^3} \left(G I_j(x_j) - x_j G II_j(x_j) - \right. \right. \\ \left. \left. \frac{x_j^2}{2} G III_j(x_j) \right) \right]. \end{aligned} \quad (3.33)$$

We consider a system for which the background plasma components have an isotropic Maxwellian distribution, namely

$$f_j(\mathbf{v}_j) = \left(\frac{m_j}{2\pi k T_j} \right)^{3/2} \exp\left(-\frac{m_j \mathbf{v}_j^2}{2k T_j} \right). \quad (3.34)$$

Moreover, the function $G_j(x_j)$ can be written in terms of error function [49]

$$G_j(x_j) = \left(x_j + \frac{1}{2x_j} \right) \text{erf}(x_j) + \frac{1}{2} \frac{d}{dx_j} \text{erf}(x_j), \quad (3.35)$$

where

$$\text{erf}(x_j) = \frac{2}{\pi^{1/2}} \int_0^{x_j} e^{-\zeta^2} d\zeta.$$

Furthermore, we assume that the energetic test particles have the velocity range as given below

$$v_{\text{bulk ions,thermal}} \ll v_b < (<) v_{e,\text{thermal}}$$

Therefore, we can apply the following asymptotic approximation of $G_j(x_j)$

$$G_{bulk\ ions}(x_i) = x_i + \frac{1}{x_i} - \frac{e^{-x_i^2}}{2\sqrt{\pi}x_i^4} \left(1 - \frac{3}{x_i^2} + \dots\right) \text{ for bulk ions } (x_i \gg 1)$$

and, respectively

$$G_e(x_e) = \frac{2}{\pi^{1/2}} \left(1 + \frac{x_e^2}{3} - \frac{x_e^4}{30} + \dots\right) \text{ for plasma electrons } (x_e \ll 1).$$

These approximations are valid to get exceptional results in fusion plasmas, where such scenarios are found quite often. For example the ions generated by Neutral beam injection (NBI) and Ion cyclotron resonance heating (ICRH) as well as for charged fusion products. The Eq. (3.33) which is the Fokker-Planck collision term can now be simplified to the form

$$\begin{aligned} \left(\frac{\partial n_b(\mathbf{r}, \mathbf{v}_b, t)}{\partial t}\right) = & \sum_{i \in (bulk\ ions)} \left(\frac{Z_b Z_i e^2}{4\pi\epsilon_0}\right)^2 \frac{2\pi n_i(\mathbf{r}) \ln \Lambda_{b,i}}{m_b^2} \left\{ \frac{2m_b}{m_i} \frac{1}{v_b^2} \frac{\partial n_b}{\partial v_b} + \frac{v_{i,thermal}^2}{v_b^3} \frac{\partial^2 n_b}{\partial v_b^2} \right\} + \\ & \left(\frac{Z_b e^2}{4\pi\epsilon_0}\right)^2 \frac{2\pi n_e(\mathbf{r}) \ln \Lambda_{b,e}}{m_b^2} \frac{4}{3\sqrt{\pi}v_{e,thermal}} \left\{ \frac{2m_b}{m_e v_{e,thermal}^2} \left[3n_b + v_b \frac{\partial n_b}{\partial v_b} \right] + \right. \\ & \left. \frac{\partial^2 n_b}{\partial v_b^2} \right\}. \end{aligned} \quad (3.36)$$

From the above relation we can see that for an isotropic background plasma system the collisions show no effect on any other change in the distribution of slowing down except the change in speed v_b . Another simplification can be employed, which gives the definition of two distinctive parameters. One is the Spitzer-slowning down time which has the mathematical form [50]

$$\tau'_s := \left(\frac{4\pi\epsilon_0}{Z_b e^2}\right)^2 \frac{3m_b m_e v_{e,thermal}^3}{16\sqrt{\pi}n_e \ln \Lambda_{b,e}} = \left(\frac{4\pi\epsilon_0}{Z_b e^2}\right)^2 \frac{3m_b (2kT_e)^{3/2}}{16\sqrt{\pi}m_e n_e \ln \Lambda_{b,e}}, \quad (3.37)$$

and the other one is the critical velocity which is given by

$$v'_{c,i} := \left(\frac{3\sqrt{\pi}}{4} \frac{m_e}{m_i} \frac{n_i Z_i^2 \ln \Lambda_{b,i}}{n_e \ln \Lambda_{b,e}}\right)^{3/2} v_{e,thermal}. \quad (3.38)$$

Using these two definitions into the Fokker-Planck equation for Coulomb collisions with an isotropic Maxwellian background plasma, we find

$$\left(\frac{\partial n_b(\mathbf{r}, \mathbf{v}_b, t)}{\partial t}\right) = \frac{1}{\tau_s \nu_b^2} \frac{\partial}{\partial v_b} \left[\left\{ v_b^3 + \sum_{i \in (\text{bulk ions})} v_{e,i}^3 \right\} n_b \right] + \frac{1}{2\tau_s \nu_b^3} \left[\frac{m_e}{m_b} v_{e,thermal}^2 v_b^3 + \sum_{i \in (\text{bulk ions})} \frac{m_i}{m_b} v_{i,thermal}^2 v_{c,i}^3 \right] \frac{\partial^2 n_b}{\partial v_b^2}. \quad (3.39)$$

The first term of the above equation is known as the dynamical friction or drag and the second term is known as the velocity diffusion term.

The deceleration's time constant of the mean speed of the test particle is actually the Spitzer-slowng down time, i.e.

$$\frac{d \langle v_b \rangle}{dt} = - \frac{\langle v_b \rangle}{\tau_s}. \quad (3.40)$$

The cause of deceleration are the collisions of the test particle with the background plasma. If

$$v_b > \left(\sum_i v_{c,i}^3 \right)^{3/2},$$

it means that the leading deceleration mechanism is clearly the friction on the electrons. The slowing down on ions becomes notable for [50]

$$v_b \leq \left(\sum_i v_{c,i}^3 \right)^{3/2},$$

and this occurs at a time constant which is completely different from the Spitzer-slowng down time (τ_s).

3.2 Another derivation for mean rate of energy transfer

There is also an alternate way through which one can also derive the loss of mean energy of a suprathermal test particle as caused by the Coulomb collision. For this calculation, the same condition of an isotropic Maxwellian background plasma is used. The mean rate of energy transfer from fast ions b' to the bulk plasma species j' can be written as [51]:

$$\begin{aligned} \left\langle \frac{\Delta E_i}{\Delta t} \right\rangle_{b' \rightarrow j'} &= \left\langle \frac{dE_i}{dt} \right\rangle_{b' \rightarrow j'} (E_{b'}, T_{j'}) \\ &= -\frac{Z_{b'}^2 Z_{j'}^2 e^4}{4\pi\epsilon_0^2} \frac{n_{j'}}{m_{j'}} \sqrt{\frac{m_{b'}}{2E_{b'}}} \ln \Lambda_{b',j'} \mathbf{F}_{j'} \left(\sqrt{\frac{m_{j'} E_{b'}}{m_{b'} k T_{j'}}}, \frac{m_{j'}}{m_{b'}} \right), \end{aligned} \quad (3.41)$$

where

$$\mathbf{F}(x', \beta') = \text{erf}(x') - (1 + \beta') x' \frac{d}{dx'} \text{erf}(x') = \frac{2}{\sqrt{\pi}} \int_0^{x'} e^{-\zeta'^2} d\zeta' - (1 + \beta') \frac{2x'}{\sqrt{\pi}} e^{-x'^2}. \quad (3.42)$$

Now we use the asymptotic approximations for small and large values of arguments of $\mathbf{F}(x', \beta')$ [52]

$$\mathbf{F}(x', \beta') \approx \frac{2}{\sqrt{\pi}} \left[-\beta' x' + \left(\frac{2}{3} + \beta' \right) x'^3 + \dots \right], \text{ if } x \ll 1, \text{ explicitly for } E_{b'} \ll kT_e \frac{m_{b'}}{m_e},$$

and

$$\mathbf{F}(x', \beta') \approx \frac{2}{\sqrt{\pi}} \left[\frac{\sqrt{\pi}}{2} - \dots \right] = 1, \text{ if } x \gg 1, \text{ explicitly for } E_b > (>) kT_i m_{b'}/m_i,$$

which provides

$$\left\langle \frac{dE}{dt} \right\rangle_{b' \rightarrow e} = -\frac{Z_{b'}^2 e^4}{3\sqrt{2}\pi^3 \epsilon_0^2} \frac{\sqrt{m_e}}{m_{b'}} n_e \ln \Lambda_{b' \rightarrow e} (kT_e)^{-3/2} E_b(t), \quad (3.43)$$

and, respectively

$$\left\langle \frac{dE}{dt} \right\rangle_{b' \rightarrow \text{bulk ions}} = -\frac{Z_{b'}^2 e^4 \sqrt{m_{b'}}}{4\pi\sqrt{2}\epsilon_0^2} \sum_{i \in (\text{bulk ions})} \frac{n_i Z_i^2 \ln \Lambda_{b' \rightarrow i}}{m_i} E_{b'}^{-1/2}(t). \quad (3.44)$$

Thus, we obtain the same results for the degradation of the mean energy of a test particle due to Coulomb collision in a Maxwellian distribution of background plasma.

3.3 Energy transfer (from zero to maximum)

The zero energy transfer between a test particle and a bulk particle can be studied by simply considering

$$\mathbf{F}'_j \left(\sqrt{\frac{m'_j}{2kT'_j}}, \frac{m'_j}{m'_b} \right) = \mathbf{F}(x'_j, \beta'_j) = 0.$$

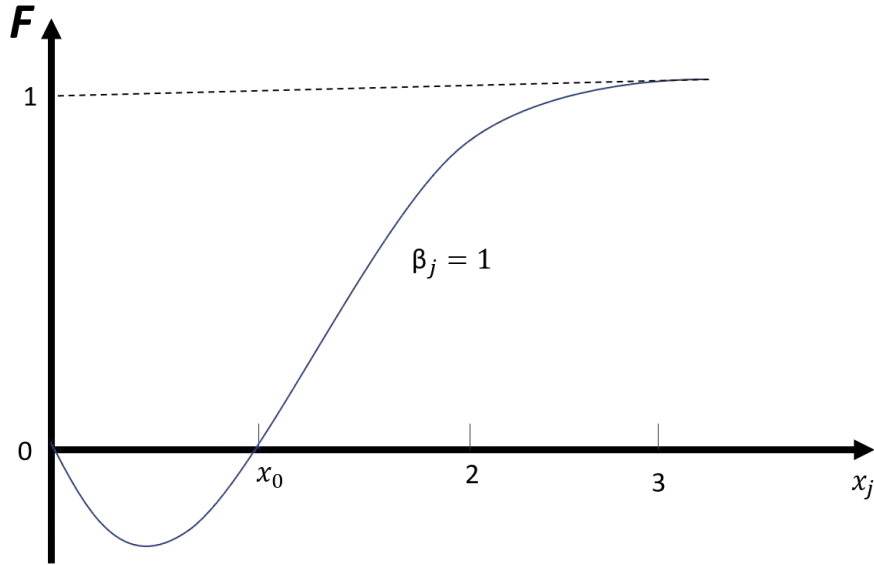


Figure 3.2: Graph for zero and maximum energy transfer.

$$\left\langle \frac{dE'_b}{dt} \right\rangle_{b \leftrightarrow j} = 0 \rightarrow \mathbf{F}(x'_0, \beta'_j) = 0 \rightarrow 1 + \beta'_j = \frac{e^{x'^2_0}}{x'_0} \int_0^{x'_0} e^{-\zeta'^2} d\zeta' \Rightarrow x'_0 \quad (3.45)$$

If we take $v'_b = v_0 = x'_0 \sqrt{\frac{2kT'_j}{m'_j}}$, there is almost zero energy transfer between the test particle b and remaining particles j . For $v'_b > v_0$, the test particle transfers energy to the particles j . Finally, if $v'_b < v_0$, the fast particle b gains energy from the background plasma particles j in collisions.

The condition for which energy transfer is maximum is $\frac{\partial \mathbf{F}(x_j, \beta_j)}{\partial x_j} = 0$

$$\Rightarrow 1 + 2x_m^2(1 + \beta_j) = \frac{e^{x_m^2}}{x_m} \int_0^{x_m} e^{-\zeta^2} d\zeta. \quad (3.46)$$

To get some insight, we make the following three cases of β_j , namely

$$\beta_j = \frac{m_j}{m_b} \begin{cases} \ll 1 \\ \approx 1 : \\ \gg 1 \end{cases}$$

Case A: $\beta_j \ll 1$, interaction among fast ions b with background electrons $\rightarrow x_0^2 = \frac{3}{2}\beta_j$;

$$\begin{aligned} \Rightarrow x_m &\approx x_m(\beta_j = 0) + \frac{x_m(\beta_j = 0)}{2[x_m^2(\beta_j = 0) - 1]}\beta_j + \dots \\ &= 1, 52 + 0, 580\beta_j - 0, 458\beta_j^2 + 0, 57\beta_j^3 + \dots \end{aligned} \quad (3.47)$$

Case B: $\beta_j \gg 1$, beam of electrons is injected into the plasma,

$$\rightarrow x_0^2 \approx \ln A + \frac{1}{2} \ln \left(\ln A + \frac{1}{2} \ln \ln A \right);$$

$$\Rightarrow x_m^2 \approx \ln(2A) + \frac{3}{2} \ln \left(\ln(2A) + \frac{3}{2} \ln \ln(2A) \right), \quad (3.48)$$

where

$$A = \frac{2}{\sqrt{\pi}}(1 + \beta_j). \quad (3.49)$$

As an example we have the case of interaction of energetic electrons with plasma deuterons, for which case $x_0 = 3.0, 7.0$ and $x_m = 3.0, 58.0$.

Case C: $\beta_j \approx 1$, interaction between beam of ions and ions, $\rightarrow x_0 \approx 1$;

$$\Rightarrow v_0 \approx \sqrt{\frac{2kT_j}{m_j}}; x_m \approx 1.0, 85.0, \quad (3.50)$$

$$\Rightarrow E_0 = \frac{mv_0^2}{2} = \frac{x_0^2}{\beta_j} kT_j; E_m = \frac{mv_m^2}{2} = \frac{x_m^2}{\beta_j} kT_j. \quad (3.51)$$

Before having a chance to look into it carefully, it seems like an ambiguity that here $E_0 \neq \frac{3}{2}kT_j$. Only the case A, in which $\beta_j \ll 1$, there is zero energy transfer. In this case, E_0 approaches the value $\frac{3}{2}kT_j$. In the remaining two cases $E_0 < \frac{3}{2}kT_j$. The logic behind $E_0 < \frac{3}{2}kT_j$ is the assumption that we made. In this assumption we have only considered the collisional interaction of a monoenergetic ion beam. For such a beam, the rate of energy transfer at $E_b = \frac{3}{2}kT_j$ does not vanish. There is only one condition which results in $E_0 = \frac{3}{2}kT_j$. According to this condition, both the interacting species should have the isotropic Maxwellian distribution of the velocities with equal temperature.

3.4 Time of Thermalization

The time required for fast particle to get slow down from its birth energy E_{birth} to thermal energy can be calculated straightforwardly by the relation [53]

$$\tau'_{thermal} = \int_0^{\tau'_{thermal}} dt = \int_{E_{birth}}^{E_{cut\ off}} \frac{dt}{dE_b} dE_b \approx \int_{3kT}^{E_{birth}} \left| \left\langle \frac{dE}{dt}(E_b) \right\rangle \right|^{-1} dE_b, \quad (3.52)$$

whereas $E_{cut\ off} \approx (1, 2.5)E_{thermal} \approx 3kT_{i(e)}$. From Eq. (3.52) time of thermalization can be evaluated as

$$\tau'_{thermal} = \frac{\tau'_s}{3} \ln \left[\frac{1 + (E_{birth}/E_c)^{3/2}}{1 + (E_{cut\ off}/E_c)^{3/2}} \right], \quad (3.53)$$

where E_c represents the critical energy, at which the Coulomb drag on the interacting electrons and bulk plasma ions becomes equal. It is very simple to calculate the value of E_c ,

we presume that

$$\frac{m_b}{m_i} kT_i \ll E_c \leq \frac{m_b}{m_e} kT_e.$$

The above-mentioned assumption decreases the value of denominator in the logarithm term of Eq. (3.53) approximately to unity. As a result we get the following expression for E_c

$$E_c = 1.2 \frac{m_b}{m_e} kT_e \left(\frac{m_e}{n_e} \sum_i \frac{n_i Z_i^2}{m_i} \right)^{2/3}. \quad (3.54)$$

The exclusion of energy diffusion in this model, of slowing down of particles, introduces some errors of the order of $kT_{i(e)}/E_0$. This can be neglected without any loss while doing the calculations when the below given approximation is used

$$\frac{E_b}{E_m} \geq \frac{3kT_i}{2m_i}.$$

It is made clear by using examples in the figures which exhibit that the portion of injected beam power, y_I , and, respectively, of the power discharged with fusion alphas, y_C that are transmitted to electrons.

Critical parameters for various values of $\beta_j = m_j / m_b$									
β	x_0	x_m	$\frac{E_0}{kT_j}$	$\frac{E_m}{kT_j}$	β	x_0	x_m	$\frac{E_0}{kT_j}$	$\frac{E_m}{kT_j}$
0	0	1.52	1.5	∞	30	2.07	2.68	0.144	0.240
0.1	0.377	1.57	1.42	24.6	40	2.15	2.75	0.115	0.189
0.2	0.519	1.61	1.35	13.0	50	2.21	2.80	0.0980	0.157
0.3	0.620	1.65	1.28	9.10	60	2.25	2.84	0.0840	0.134
0.4	0.699	1.69	1.22	7.13	70	2.28	2.87	0.0743	0.118
0.5	0.765	1.72	1.17	5.92	80	2.31	2.90	0.0670	0.105
0.6	0.822	1.75	1.12	5.10	90	2.34	2.92	0.0612	0.0950
0.7	0.871	1.78	1.08	4.53	100	2.37	2.94	0.0556	0.0867
0.8	0.915	1.81	1.05	4.10	200	2.52	3.08	0.0317	0.0478
0.9	0.954	1.83	1.01	3.73	300	2.60	3.15	0.0226	0.0332
1.0	0.990	1.85	0.980	3.42	400	2.66	3.21	0.0177	0.0258
1.1	1.02	1.87	0.948	3.18	500	2.71	3.25	0.0147	0.0211
1.2	1.05	1.89	0.918	2.99	600	2.74	3.28	0.0125	0.0180
1.3	1.08	1.91	0.897	2.80	700	2.77	3.31	0.0110	0.0157
1.4	1.11	1.93	0.873	2.65	800	2.80	3.33	0.00980	0.0139
1.5	1.13	1.94	0.852	2.51	900	2.82	3.35	0.00887	0.0125
2	1.23	2.01	0.757	2.03	1 000	2.84	3.37	0.00807	0.0114
3	1.37	2.11	0.626	1.49	2 000	2.97	3.49	0.00441	0.00608
4	1.47	2.18	0.541	1.19	3 000	3.04	3.55	0.00308	0.00421
5	1.54	2.24	0.475	1.01	4 000	3.09	3.60	0.00239	0.00322
6	1.60	2.29	0.427	0.875	5 000	3.13	3.63	0.00196	0.00264
7	1.65	2.33	0.388	0.775	6 000	3.16	3.66	0.00165	0.00223
8	1.69	2.36	0.357	0.697	7 000	3.18	3.68	0.00145	0.00194
9	1.73	2.39	0.331	0.635	8 000	3.20	3.70	0.00128	0.00172
10	1.76	2.42	0.310	0.585	9 000	3.22	3.72	0.00116	0.00154
15	1.88	2.52	0.235	0.423	10 000	3.24	3.74	0.00105	0.00140
20	1.96	2.59	0.193	0.335					

Figure 3.3: Table showing the behavior of x_0 , x_m , $\frac{E_0}{kT_j}$, and $\frac{E_m}{kT_j}$ for different values of $\beta_j = \frac{m_j}{m_0}$. It can be seen that that by increasing the value of β_j from 0 to 20 in different steps x_0 and x_m goes on increasing and the values of $\frac{E_0}{kT_j}$ and $\frac{E_m}{kT_j}$ goes on decreasing. As soon as we increase the value of β_j from 30 to 10,000, the numerical values of x_0 and x_m start decreasing, and the values of $\frac{E_0}{kT_j}$ and $\frac{E_m}{kT_j}$ keep decreasing. By taking highly energetic ions into consideration created by, for example NBI, it can be observed that $\left\langle \frac{dE}{dt} \right\rangle_{b \rightarrow e}$ surpasses

$\left\langle \frac{dE}{dt} \right\rangle_{b \rightarrow \text{bulk ions}}$ by far.

3.5 Equilibrium temperature of a two-component plasma

In a plasma having two components the equilibrium temperature can be obtained as follows:

One of the components is bulk plasma particles and the other one is test particles. The bulk plasma particles have a Maxwellian distribution at temperature T_j with mass m_j and charge Z_j . The test particles also follow the Maxwellian distribution at temperature T_k with mass m_k and charge Z_k , respectively. Our purpose is to find the mean rate of energy transfer from a test particle to all the bulk particles j .

The mean rate of energy transfer can be calculated by averaging as

$$\begin{aligned}
 P_{k \rightarrow j} &= \left| \left\langle \frac{dE_k}{dt} \right\rangle_{k \rightarrow j} \right| = \frac{Z_k^2 Z_j^2 e^4 n_j}{4\pi\epsilon_0^2 m_j} \sqrt{\frac{m_k}{2E_k}} \ln \Lambda_{kj} \mathbf{F}_j \left(\sqrt{\frac{m_j E_k}{m_k k T_j}}, \frac{m_j}{m_k} \right) \\
 &= \frac{Z_k^2 Z_j^2 e^4 n_j}{4\pi\epsilon_0^2 m_j} \frac{1}{v_k} \ln \Lambda_{kj} \mathbf{F}_j \left(v_k \sqrt{\frac{m_j}{2kT_j}}, \frac{m_j}{m_k} \right),
 \end{aligned} \tag{3.55}$$

over the distribution function of the test particle denoted as $f_{DT}(v_k)$. In simple words our main goal is to get the Maxwellian average

$$\langle P_{k \rightarrow j} \rangle_{DT} = \int P_{k \rightarrow j} f_{DT}(v_k) d^3 v_k. \tag{3.56}$$

The above expression, in more simplified form, can be written as

$$\left\langle \frac{\mathbf{F}_j}{v_k} \right\rangle_{DT} = \left\langle \frac{\text{erf}(v_k b_j)}{v_k} \right\rangle_{DT} - K \langle e^{-b_j^2 v_k^2} \rangle_{DT}, \tag{3.57}$$

whereas $b_j = \sqrt{\frac{m_j}{2kT_j}}$ and K is a constant which is self-explanatory.

3.6 Results and Discussion

Now we are going to plot some of the equations derived above and discuss the results. Figure (3.4) explains the relative part of energy of injected particles transferred to electrons and ions respectively, and the absolute value of energy received by the ions. The break even point between absorption of two species can be observed at 44 keV. We must know that for

higher injection energies, even though the part of energy taken by the electrons decreases, the full amount of energy transferring to the ions enhances till it asymptotes about 0.07 MeV. Thus, it shows an optimum injection energy. Figure (3.5) shows the behavior of alpha

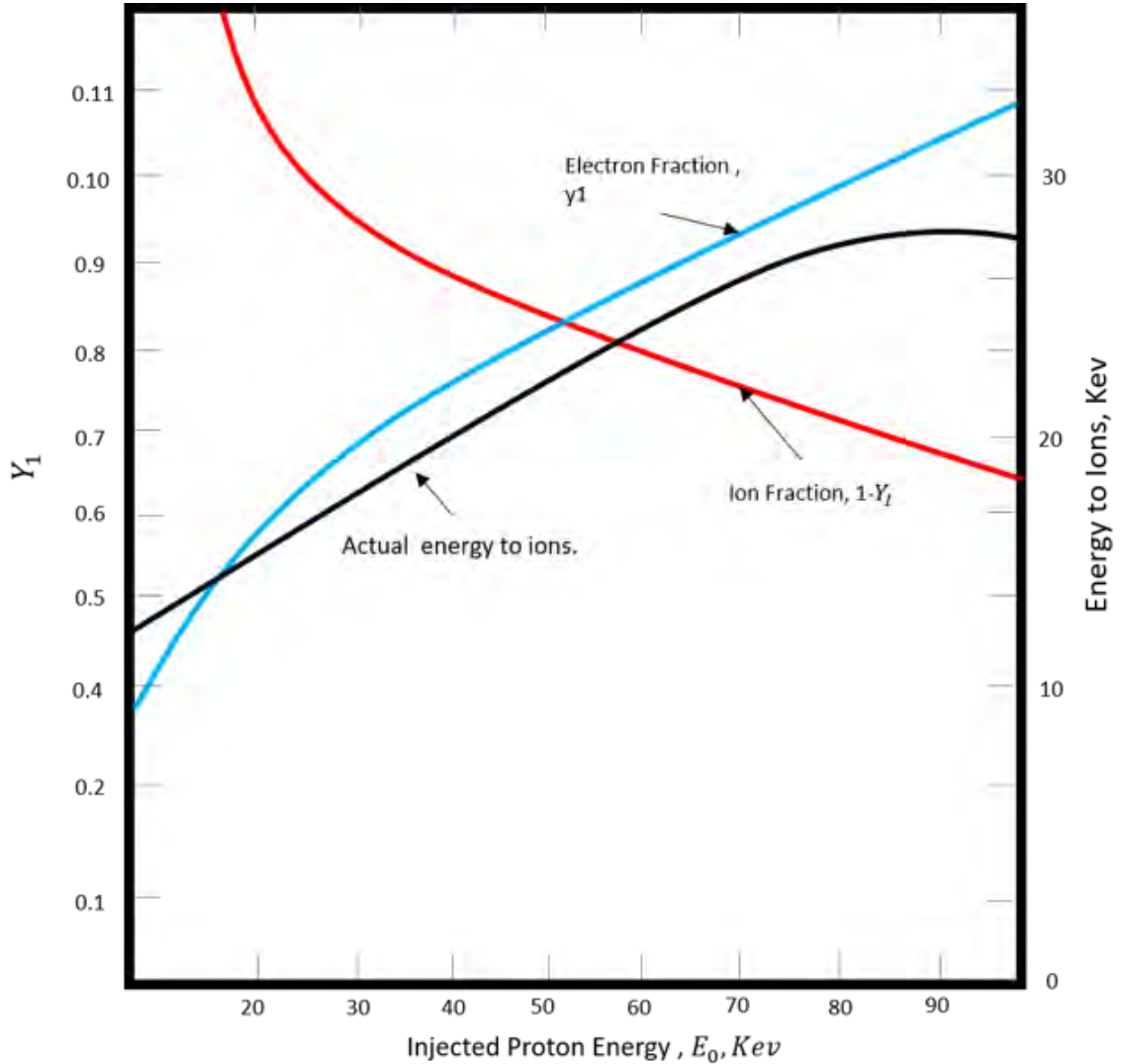


Figure 3.4: The curves in color red and blue show the fraction of injected ion energy which is transferred to electrons and ions in a tokamak-like plasma vs injection energy. (Use LHS scale.) The absolute value of injected particle energy transferred to the ions of plasma is shown by the curve color black. (Use RHS scale.) ($n = 5 \times 10^{13} \text{cm}^{-3}$, $T_e = 1 \text{ keV}$, and $T_i = 0.5 \text{ keV}$.)

particle which transfers the relative quantity of energy to electrons and ions respectively in a tokamak-like plasma with electron temperature on x-axis. At $T_e = 45 \text{ keV}$, there lies the point, namely, break even point between the two species (electron and ion) absorption. As

cooling on one specie (electron) means a robust sink of energy for the other specie (ions), thus, enhancing the T_e above 45 keV is advantageous. The energy required to heat up the electrons can be regained from the enhanced fusion energy outcome.

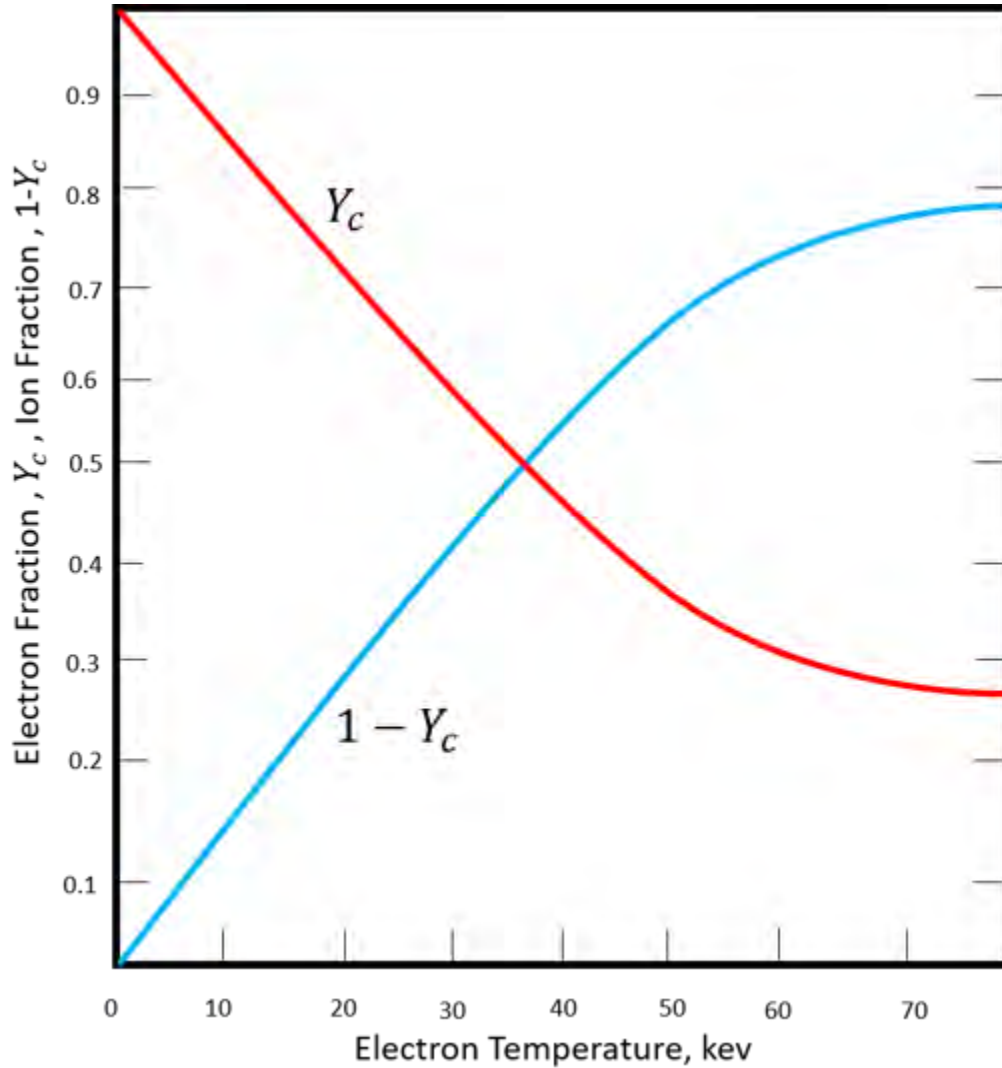


Figure 3.5: The curve color red shows the fraction of electrons and the curve color blue shows the fraction of ions receiving the energy of the alpha particle vs the temperature of electrons in a common deuterium-tritium plasma with $T_i = T_e$.

The temperature required for an alpha particle to relax in a tokamak is much less than the ion temperature as compared to a mirror machine. Explicitly, it is calculated for $n = 10^{14} \text{cm}^{-3}$, $T_e = 7 \text{ keV}$, $T_i = 5 \text{ keV}$ and quantity of deuterium and tritium is equal. It is measured that an alpha particle takes 250 msec to decrease its energy from 3.5 MeV to 0.012 MeV. The energy's 87 % is taken by electrons and the remaining 13% is taken by

ions. This numerical value for the thermalization time is greater than the present plasma lifetimes. It can be noted that the ions are still getting an energy of 0.4 MeV which is the hundred times of their mean energy. Moreover, concluding remarks on alpha particles heating of tokamaks cannot be given unless trustworthy buildup and loss models have been given. For tokamak heating via injection of energetic neutral particles, the slowing-down of a proton is calculated.

In fig.(3.6) $\tau_0 = f(E_0)$ is plotted against E_0 for many numerical values of the electron temperature (T_e). These results are obtained by presuming hydrogen ion injection into a hydrogen plasma. It can be seen that by increasing the value of electron temperature the slowing down time increase. Because by increasing the temperature, number of collisions also increases. Thus, the time required to slow down the particles increases. Moreover, with increasing values of E_0 the slowing down time becomes constant.

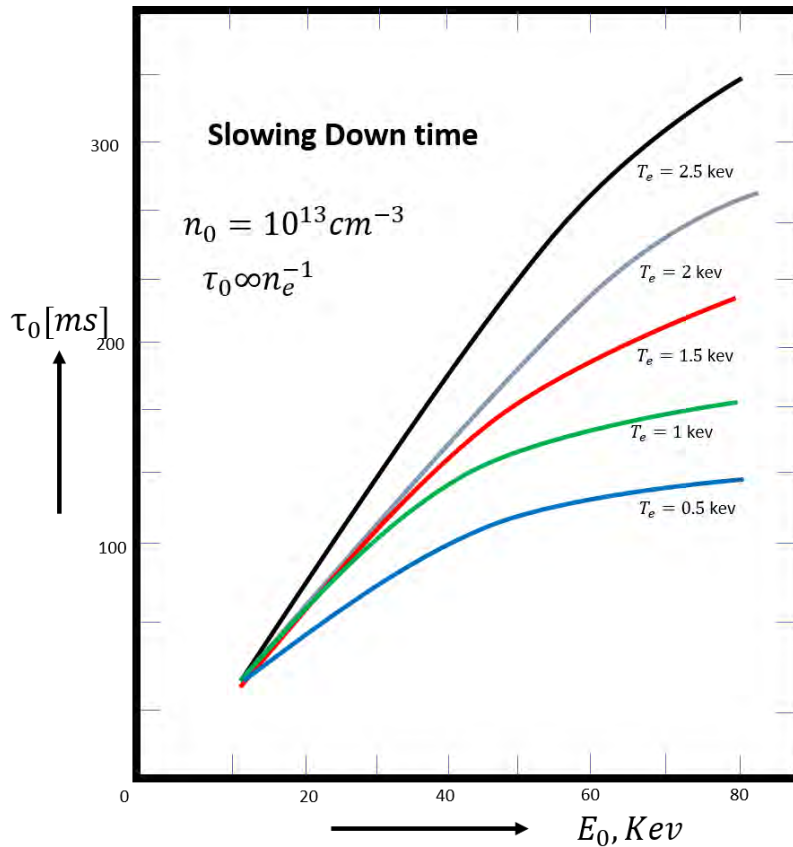


Figure 3.6: In a hydrogen plasma, slowing-down time of hydrogen ions is plotted with respect to energy of ion at different values of the electron temperature (T_e).

In fig.(3.7) the slowing-down velocity $\frac{dE}{dt}$ is plotted against E_0 for many numerical values of the electron temperature (T_e). These results are obtained by assuming hydrogen ion injection into a hydrogen plasma. It can be seen that by increasing the value of electron temperature the slowing down velocity $\frac{dE}{dt}$ decreases. With increasing values of E_0 the slowing down velocity approaches a constant value. At lowest electron temperature $T_e = 0.5$ keV, there is a sudden rise in the slowing down velocity. It happens because of decrease in number of collisions with decreasing temperature. Also, the slowing down velocity is directly proportional to the number density of the particles. The minimum of slowing down velocity occurs at $E = 1/(2)^{2/3}E_c$. In terms of electron temperature, the value of energy at which this minimum appears is $E \simeq 10T_e$. In Fig. (3.8) it is shown that

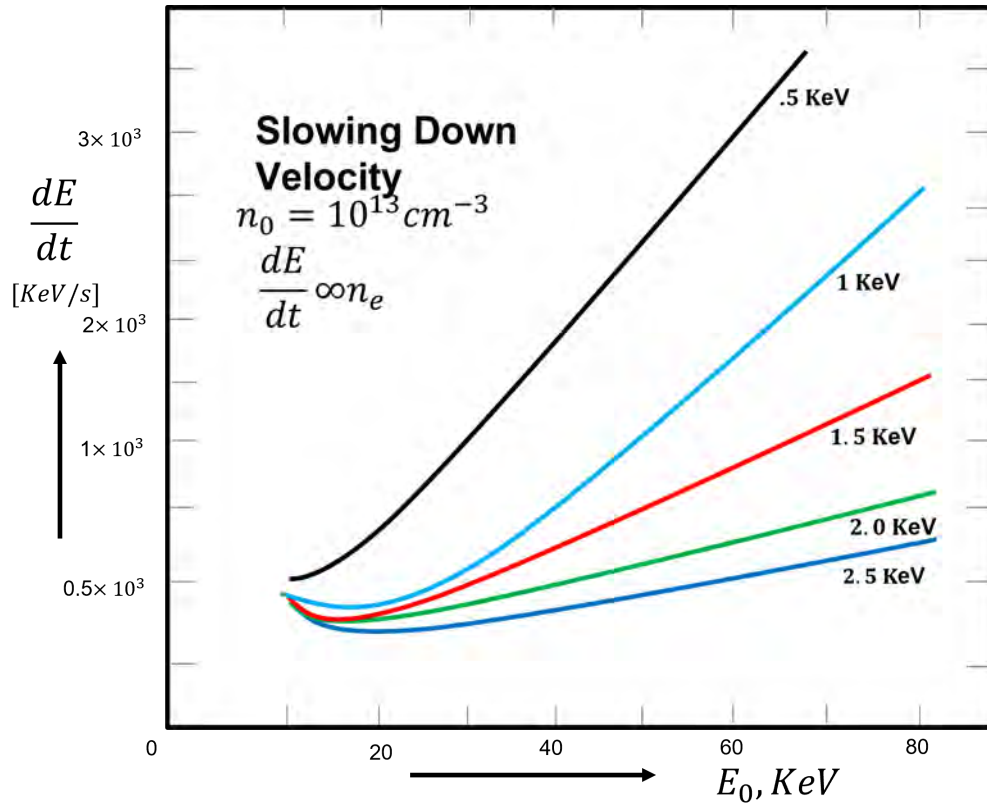


Figure 3.7: In a hydrogen plasma, slowing-down velocity of hydrogen ions is plotted with respect to energy of ion at different values of the electron temperature (T_e).

how the relative particle losses depend on ratio of the number density of the particles for many values of electron temperature T_e and energy E_0 . It is assumed that the hydrogen ions are injected into the hydrogen plasma with $A = A_i = 1$. To keep the things simple, for each

case $T_i = 1$ keV is chosen. It is estimated that the values of neutral background densities n_0 in current tokamaks is about 10^{-8} cm $^{-3}$ [54]. It means that the ratio of the densities is in the range 10^{-5} , if the plasma densities n_e included are not high enough. In this regard, however, the curves in Fig. (3.8) are actively show an enhancing behavior. Thus, particle losses and its correlated effects (energy losses etc.) cannot be ignored.

The above results are also valid for cases where hydrogen isotopes are injected into the plasma containing (mainly) hydrogen isotopes. To do this, the parameters n_0/n_e , T_e , E_0 and T_i must be properly re-defined. The results shown in the figure. (3.8) can be modified for any combination of $A \neq 1$ and/or $A_i \neq 1$ by replacing the abscissa and curve parameters. These modifications are also valid if the plasma contains a mixture of two or more hydrogen isotopes. But only one isotope must maintain dominance, $Z \simeq Z_H \simeq 1$. For example, we might consider deuterium injection into deuterium plasma. Particle deficits are equivalent to the case of hydrogen ion injection into hydrogen plasma if the following conditions are met: $(n_0/n_e)_D = 0.25(n_0/n_e)_H$, $T_{eD} = 2^{2/3}T_{eH}$, $E_{0D} = 2E_{0H}$ and $T_{iD} = 2T_{iH}$. In case of $E_0 \gg T_i$, the T_i dependency can be ignored. It is fascinating to understand that in order to obtain the same particle losses, it is necessary to reduce the neutral density by a factor of 4.

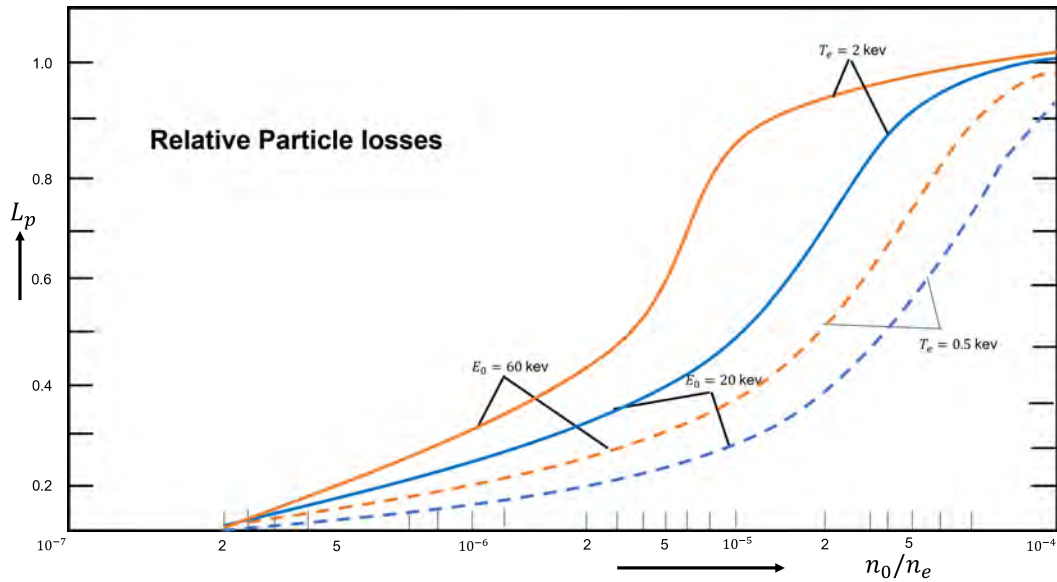


Figure 3.8: In a hydrogen plasma with hydrogen ions injected, the behavior of relative particle loss (L_p) against the ratio of neutral background density to plasma density n_0/n_e is shown for many numerical values of energies and electron temperatures.

Figure (3.9) shows some graphs for relative energy losses as a function of the ratio of number density of the particles. These graphs are plotted according to the assumptions $A = A_i = 1$ and hydrogen ion injection into a hydrogen plasma. All other parameters are same as in Fig. (3.8). It can be seen that the relative energy losses for $E_0 = 60$ keV are somewhat lower as compared to $E_0 = 20$ keV. This behavior can be understood from the fact that the slowing down velocity actively reduces with enhancing energy if the condition $E \gtrsim 20$ keV. Therefore, highly energetic ions are basically lost to plasma particles after giving them most of their energy.

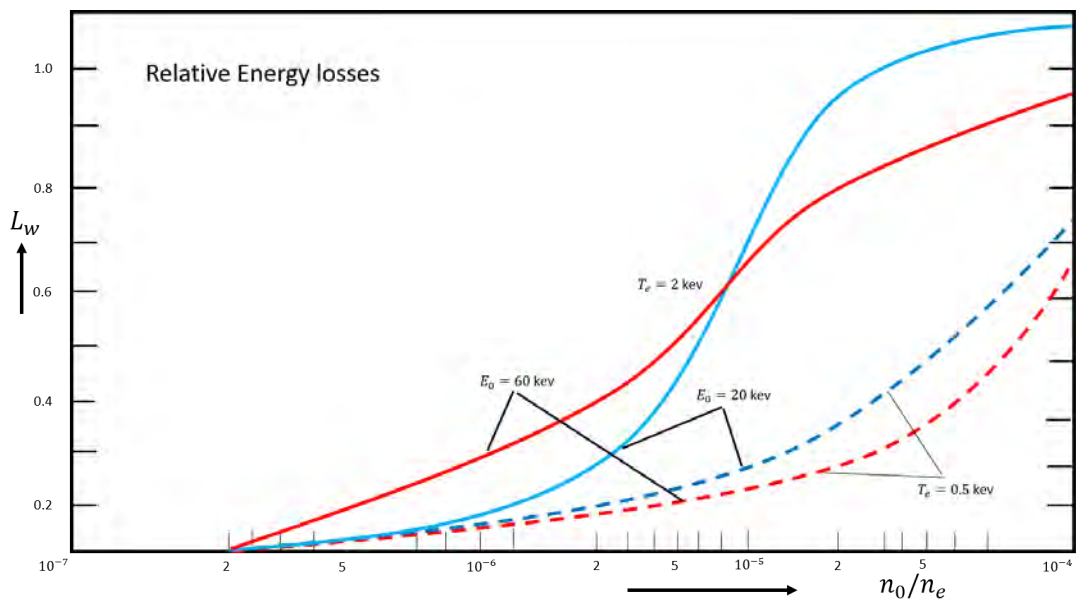


Figure 3.9: In a hydrogen plasma with hydrogen ions injected, the behavior of relative energy losses against the ratio of neutral background density to plasma density is shown for many numerical values of energies and electron temperatures.

Bibliography

- [1] W. W. Heidbrink, R. Kaita, H. Takahashi, G. Gammel, G. W. Hammett, and S. Kaye, *Phys. Fluids* 30, 1839 (1987).
- [2] W. W. Heidbrink, J. Kin, and R. J. Groebner, *Nucl. Fusion* 28, 1897 (1988).
- [3] W. W. Heidbrink, *Phys. Fluids B* 2, 4 (1990).
- [4] K. Tobita, K. Tani, Y. Kusama, T. Nishitani, Y. Ikeda, Y. Neyatani, S. V. Konovalov, M. Kikuchi, Y. Koide, K. Hamamatsu, H. Takeuchi, and T. Fujii, *Nucl. Fusion* 35, 1585 (1995).
- [5] M. Isobe, K. Tobita, T. Nishitani, Y. Kusama, and M. Sasao, *Nucl. Fusion* 37, 437 (1997).
- [6] L. Zhao, W. W. Heidbrink, H. Boehmer, R. McWilliamms, D. Leneman, and S. Vincena, *Phys. Plasmas* 12, 052108 (2005).
- [7] N. Rostoker, *Nucl. Fusion* 1, 101 (1961).
- [8] N. Rostoker, *Phys. Fluids* 7, 479 (1964).
- [9] D. Li, *Nucl. Fusion* 41, 631 (2001).
- [10] J. D. Strachan, P. L. Colestock, S. L. Davis, D. Eames, P. C. Efthimion, H. P. Eubank, R. J. Goldston, L. R. Grisham, R. J. Hawryluk, J. C. Hosea, J. Hovey, D. L. Jassby, D. W. Johnson, A. A. Mirin, G. Schilling, R. Stooksberry, L. D. Stewart, and H. H. Towner, *Nucl. Fusion* 21, 67 (1981).

- [11] J. Wesson, Tokamaks, Oxford Science Publication, 3rd edition (2004).
- [12] Conn, RW, On the development of fusion power **100**, 139 (1981).
- [13] Sips, ACC and Giruzzi, G and Ide, S and Kessel, C and Luce, TC and Snipes, JA and Stober, JK and Integrated Operation Scenario Topical Group of the ITPA, Progress in preparing scenarios for operation of the International Thermonuclear Experimental Reactor **22**, 021804 (2015).
- [14] K. Ikeda, Progress in the ITER physics basis **47**, 6 (2007).
- [15] Kazakov, Ye O and Ongena, J and Wright, JC and Wukitch, SJ and Lerche, E and Mantsinen, MJ and Van Eester, D and Craciunescu, T and Kiptily, VG and Lin, Y and others, Efficient generation of energetic ions in multi-ion plasmas by radio-frequency heating **13**, 973 (2017).
- [16] A. Fasoli¹, C. Gormenzano, H.L. Berk, B. Breizman, S. Briguglio, D.S. Darrow⁴, N. Gorelenkov, W.W. Heidbrink, A. Jaun, S.V. Konovalov, R. Nazikian, J.-M. Noterdaeme, S. Sharapov, K. Shinohara, D. Testa¹, K. Tobita¹, Y. Todo, G. Vlad and F. Zonca, Physics of energetic ions **47**, 264 (2007).
- [17] W. W. Heidbrink and G. J. Sadler, The behavior of fast ions in tokamak experiments **34**, 535 (1994).
- [18] S. J. Zweben et al., Alpha particle physics experiments in TFTR **39**, 275 (1997).
- [19] Walt and Martin, The radial diffusion of trapped particles induced by fluctuating magnetospheric fields **12**, 446 (1971).
- [20] S. J. Zweben et al., Alpha-particle physics in the tokamak fusion test reactor DT-experiment **40**, 91 (2000).
- [21] A. Fasoli et al., Physics of energetic ions **47**, 264 (2007).
- [22] K. McGuire et al., Study of high-beta magnetohydrodynamic modes and fast-ion losses in PDX **50**, 891 (1983).

- [23] S. J. Zweben et al., MHD induced alpha particle loss in TFTR **39**, 1097 (1999).
- [24] E. M. Carolipio, W. W. Heidbrink, C. B. Forest and R. B. White, Simulations of beam ion transport during tearing modes in the DIII-D tokamak **42**, 853 (2002).
- [25] E. Strumberger, S. Gunter, E. Schwarz and C. Tichmann, Fast particle losses due to NTMs and magnetic field ripple **10**, 023017 (2008).
- [26] Coppi, B and Porcelli, F, Theoretical model of fishbone oscillations in magnetically confined plasmas **57**, 2272 (1986).
- [27] Chen, Liu and White, RB and Rosenbluth, MN, Excitation of internal kink modes by trapped energetic beam ions **52**, 1122 (1984).
- [28] Petrov, M. P., et al., in Fusion Energy 1996 (Proc. 16th Int. Conf. Montréal, 1996) **1**, 261 (1997).
- [29] Petrov, M. P., et al., Studies of energetic confined alphas using the pellet charge exchange diagnostic on TFTR **35**, 1437 (1995).
- [30] Stratton, B. C., et al., Observation of sawtooth redistribution of non-thermal, confined alpha particles in TFTR DT discharges **36**, 1586 (1996).
- [31] Marcus, F. B., et al., Effects of sawtooth crashes on beam ions and fusion product tritons in JET **34**, 687 (1994).
- [32] Odblom, A and Anderson, D and Eriksson, L-G and Lisak, M, Modelling of sawtooth induced redistribution of ICRF heated minority ions **35**, 1571 (1995).
- [33] Kolesnichenko, Y.I., Yakovenko, Y.V., Kinetic description of redistribution of fast ions during sawtooth crashes in tokamaks **35**, 1579 (1995).
- [34] Budny, R.V., and McCune, D.C., and Redi, M.H., and Schivell, J., Wieland, R.M., TRANSP simulations of International Thermonuclear Experimental Reactor plasmas **3**, 4583 (1996).

- [35] Wong, K. L., et al., Excitation of toroidal Alfvén eigenmodes in TFTR **66**, 1874 (1991).
- [36] Porcelli, Francesco, Fast particle stabilisation **33**, 1601 (1991).
- [37] Campbell, D. J., et al., Stabilization of sawteeth with additional heating in the JET tokamak **60**, 2148 (1988).
- [38] McClements, K. G., Dendy, R. O., Gimblett, C. G., Hastie, R. J., Martin, T. J., Stabilization of the ideal $m=1$ internal kink by alpha particles and ICRF heated ions **35**, 1761 (1995).
- [39] R. C. Isler, Plasma Phys. Controlled Fusion **36**, 171 (1994).
- [40] W. W. Heidbrink, Fast-ion D α measurements of the fast-ion distribution **81**, 10D727 (2010).
- [41] T. H. Stix, Heating of toroidal plasmas by neutral injection **14**, 367 (1972).
- [42] C. K. Birdsall, Particle-in-cell charged-particle simulations, plus Monte Carlo collisions with neutral atoms, PIC-MCC **19**, 65, (1991).
- [43] Emanuel Parzen, On estimation of a probability density function and mode **33**, 3 (1962).
- [44] J. Ehlers, P. Geren, and R. K. Sachs, Isotropic solutions of the Einstein- Liouville equations **9**, 1344 (1968).
- [45] Charles Kittel, Herbert Kroemer, Thermal Physics. W. H. Freeman (1980).
- [46] A. A. Harms, K. F. Schoepf, G. H. Miley, D. R. Kingdon, Principles of fusion energy: an introduction to fusion energy for students of science and engineering. World Scientific (2000).
- [47] Landau L. D., Lifshitz E. M., Classical Mechanics. Oxford Pergamon (1960).
- [48] Bernard B. Hamel, Kinetic model for binary gas mixtures **8**, 418 (1965).

- [49] Andrews Larry C., Special functions of mathematics for engineers. Spie Press (1998).
- [50] Dan M. Goebel, Ira Katz, Fundamentals of electric propulsion: ion and Hall thrusters. John Wiley & Sons (2008).
- [51] Miymato K., Plasma physics for nuclear fusion. (1980).
- [52] Olver F. W. J., Asymptotic approximations and error bounds **22**, 188 (1980).
- [53] Boulegue G., Chanson P., Combe R., Felix M., Strasman P., Slowing-down of charged particles in a plasma. (1958).
- [54] Ott W., Speth E., Stähler A., Slowing-down of fast ions in a plasma: Energy transfer, charge exchange losses and wall sputtering. Max-Planck-Institut for Plasmaphysik (1977).